(A short?)Update on the Loma Linda Proton CT Project

Reinhard W. Schulte, Dr. med, Dipl. Phys
Professor of Radiation Medicine
Radiation Research Laboratories
Loma Linda University
California, USA

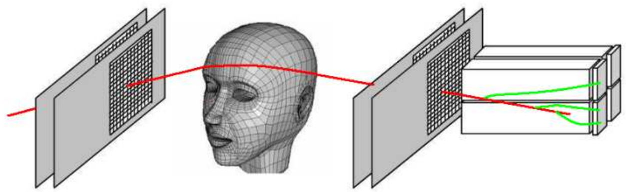

Outline

- Importance of range in particle therapy
- Proton CT (pCT) and Radiography
  - History
  - Principle of pCT and pRG
  - pCT collaboration
  - Phase 1 and 2 scanners
  - Image reconstruction
  - Proton Radiography
- Future Developments and Applications

IMPORTANCE OF RANGE IN PARTICLE THERAPY

Current Limitations of Hadron Therapy – and how to overcome them

- Biological Uncertainty: range uncertainty requires overshoot of dose, but the distal relative biological effectiveness (RBE) is least certain -> track structure studies
- Range Uncertainty: creates a conflict between healthy tissues sparing and need to completely cover tumor tissue -> proton CT
- Motion Uncertainty: position of tissues relative to the beam varies between and during treatment fractions -> image guidance with proton CT

Range Uncertainty in Particle Therapy

- Inhomogeneities are fundamentally more important in particle therapy than in X-ray therapy
- We have learned to deal with them by
  - Optimizing our X-ray CT calibration methods
  - Incorporating additional margins
  - Developing robust optimization methods for IMPRT
- We have remaining issues due to
  - Need for higher accuracy with hypofractionation and stereotactic treatments
  - Restrictions in beam entry directions
  - CT artifacts in the presence of metallic hardware, dental fillings embolization glue etc.
  - Intra- and inter-treatment changes of proton range (motion, weight loss etc.)
  - Higher RBE of distal edge when placed into critical normal tissues

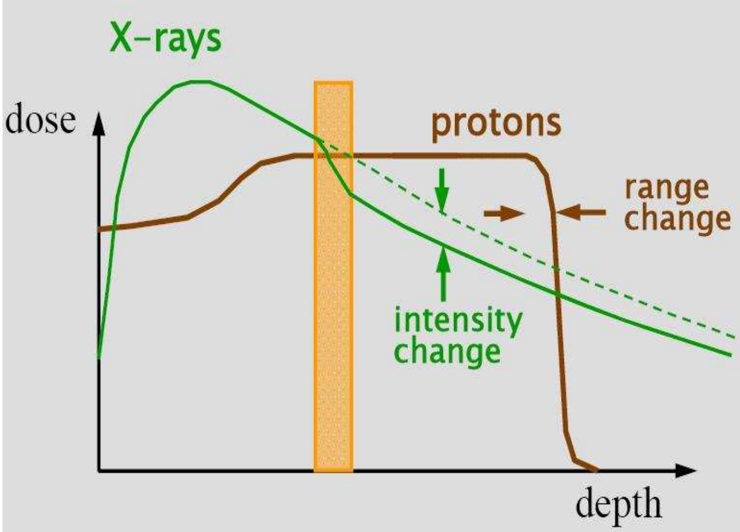

Michael Goitein, AAPM Symposium, Baltimore, May 2009

Typical Range Uncertainties in Proton Therapy – Prostate and Brain Treatments

Type of Uncertainty	Prostate	Brain
Material Densities/ Manufacture		
Bolus density	0.9 mm	0.5 mm
Bolus manufacture	0.5 mm	0.5 mm
Pod/Mask- CT conversion	1.0 mm	1.0 mm
combined	1.4 mm	1.2 mm
Patient Electron Densities	% of Range	
CT # random fluctuations	0.3 %	
Beam hardening effects	1.5 %	
HU- to rel. electron dens. conversion	2.0 %	
Combined	3.8 %	
Combined Total (GTV coverage in 90% of cases)		
Prostate (WED = 200 mm)	9 mm	
Brain (WED = 100 mm)	3 mm	

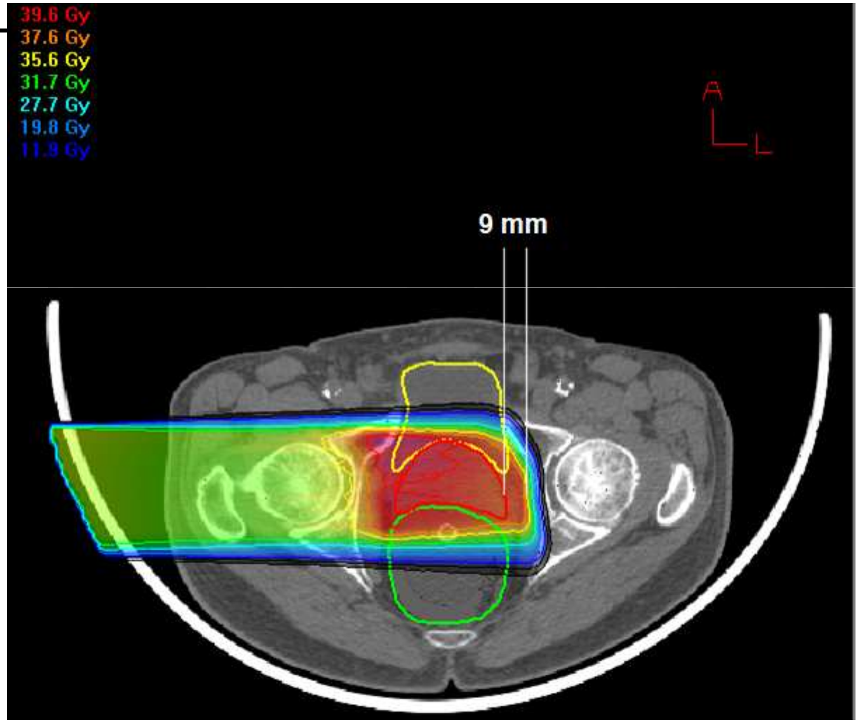

The role of CT Imaging in Charged Particle Therapy

- CT imaging is needed for
  - Target volume definition (anatomical boundaries with additional anatomical & functional information from registered MRI and PET studies)
  - Dose and range calculation
  - 3D Patient alignment verification (in-room cone beam CT, CBCT)

Pros and Cons of X-ray CT Use in Particle Therapy

- Pros
  - Widely available (diagnostic CT has firm industry support)
  - Thoroughly investigated and established
  - Excellent spatial and timing resolution
- Cons
  - Issues with conversion of CT units to relative proton stopping power, leading to systematic range errors of the order of 3-5% for soft tissues and higher for tissues with very low or high density (lung, bone) or in the presence of metal artifacts
  - Relatively high patient dose with CBCT when used as daily imaging modality for daily image verification
  - Reconstruction artifacts with MV or kV cone beam CT -> not ideal for dose replanning

Process of X-ray CT HU to Relative Stopping Power Conversion

H = 1000 $\mu^{tissue} / \mu^{water}$

RSP = $dE/dx^{tissue} / dE/dx^{water}$

CT Hounsfield values (H)

Relative proton stopping power (RSP)

Calibration curve

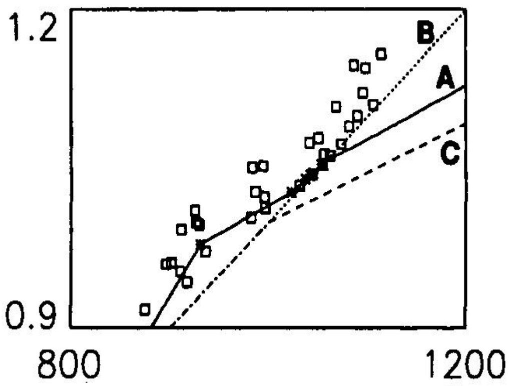

Dose & range calculation

Isodose distribution

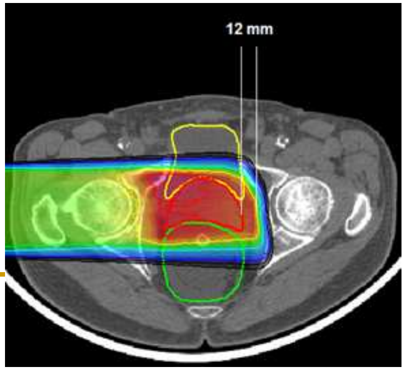

Range Accuracy of Proton/Ion Therapy when X-ray CT is used

- X-ray attenuation in the 70-120kV range is determined by photo-electric and Compton scattering
- Conversion of Hounsfield units to relative stopping power (RSP) requires careful calibration
- There is no consistent one-to-one relationship between Hounsfield units and RSP for different tissues and materials

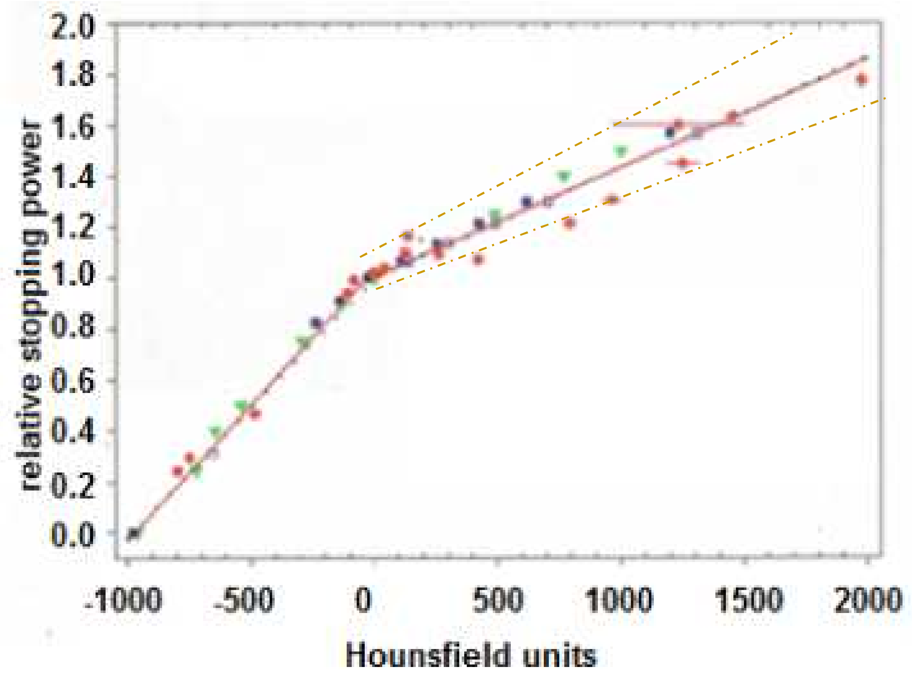

O. Jäkel, Imaging and Tumor Localization in Ion Beam Therapy, in: Ute Linz (Ed.), Ion Beam Therapy, Springer 2012)

Passive Proton Beam Delivery Technique

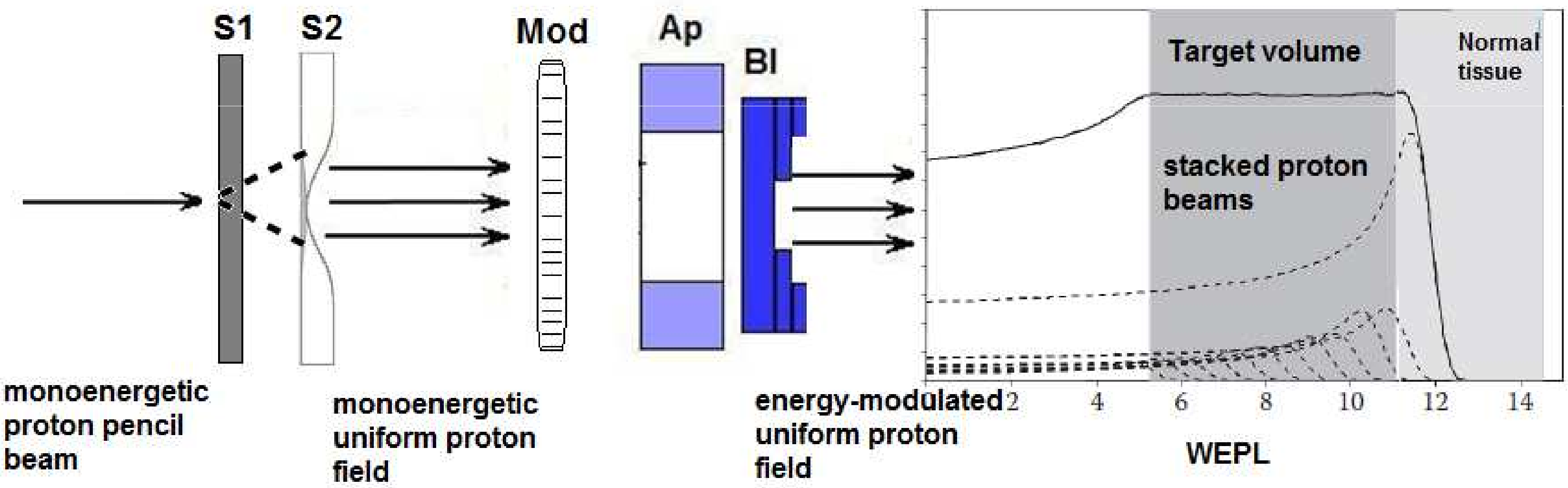

Charged Particle Treatment Planning: Proton Ray Tracing

- Protons beams are modulated in energy such that their water-equivalent pathlength in tissue places the Bragg peak at the desired location
- The most critical location is the “distal edge”
- X-ray CT provides the required WEPL data from which the required thickness of the range compensator (bolus)

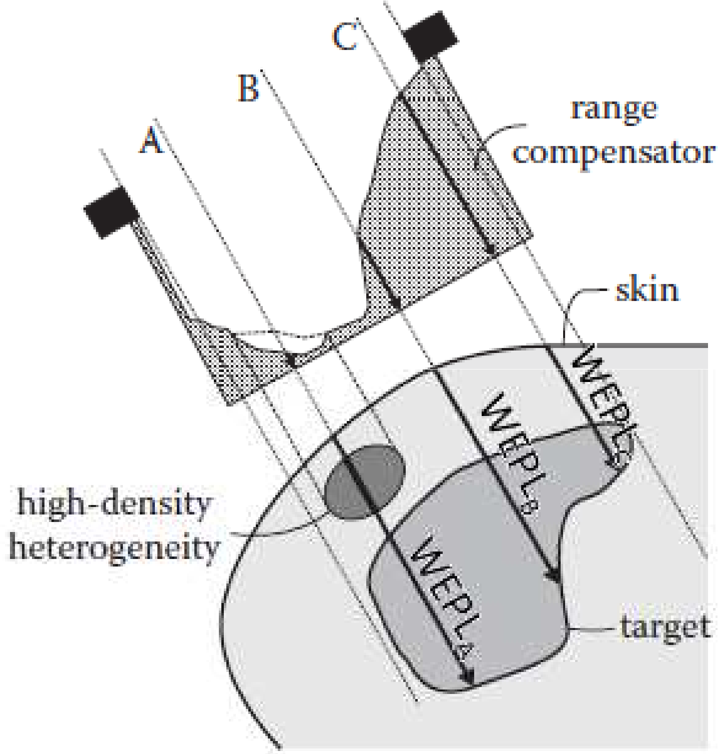

Clinical Implications of Range Uncertainties in Proton Therapy

- Differences in the interaction of x-rays and protons with matter make proton range calculations uncertain
- Range uncertainties can range from mm to cm
- Materials of unknown stopping power and CT artifacts create additional uncertainties
- The problem of range uncertainty also exists with active scanning when range error exceeds longitudinal width of Bragg peak

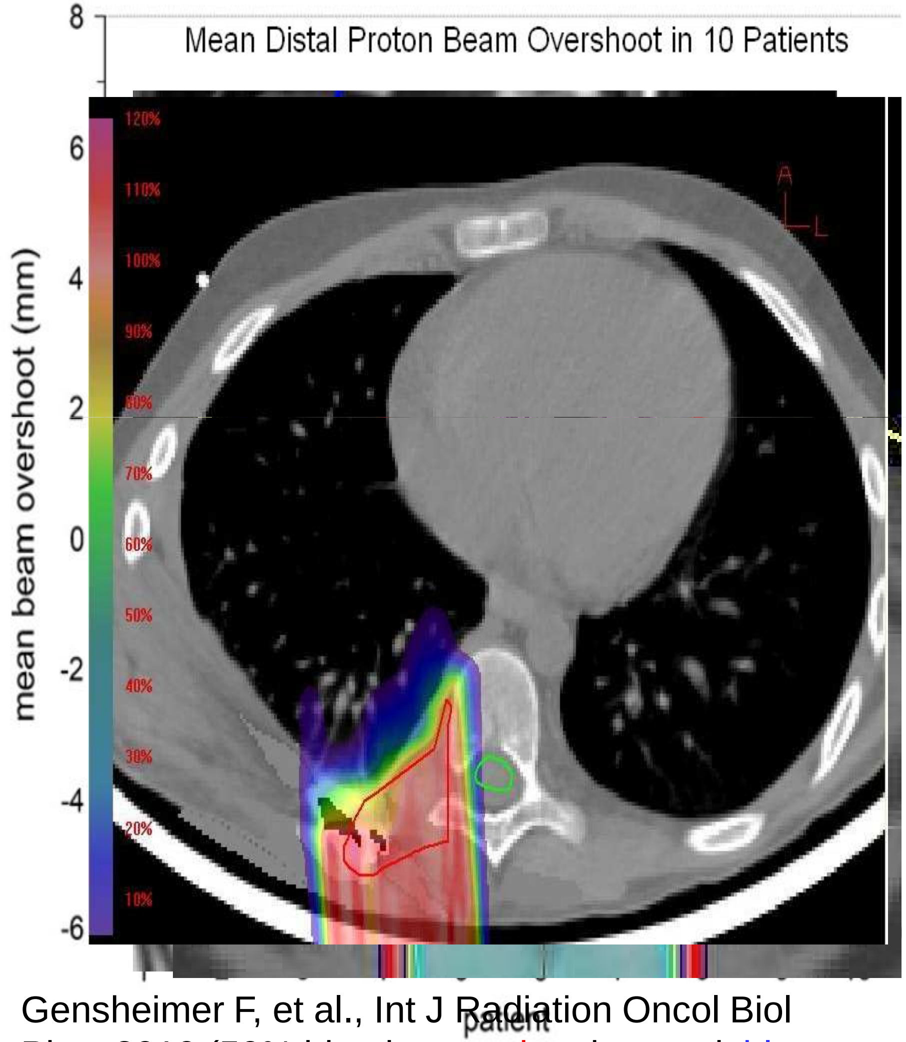

Gensheimer F, et al., Int J Radiation Oncol Biol Phys 2010 (50% idosdose, red = observed, blue = planned

Goal: Reduction of Range Errors in Particle Therapy

- Our ultimate goal in proton and ion therapy is to use proton or other light ion beams of sufficient range for treatment planning and integral range verification
- This will allow reconstruction of the volumetric distribution of relative stopping power for proton and ion treatment planning and pre-treatment verification
- First systems for proton imaging have been developed in recent years

PROTON CT AND RADIOGRAPHY: PRINCIPLE, CONCEPTS, HISTORY & REALIZATION

Principle of Proton Imaging

- Due to electronic and elastic nuclear interactions protons lose energy and acquire scattering angle variance; in addition they may be lost due to inelastic nuclear interactions
- The object can conceptually be replaced by a uniform water slab that, on average, leads to the same energy loss, difference in scattering angle variance, or loss due to nuclear interactions
- Based on this information, water equivalent pathlengths ($WEPL_{st}$, $WEPL_{sc}$), $WEPL_{ni}$ may be derived
- A 2D plot of average WEPL values per pixel produces radiographs
- Tomographic or 3D reconstruction of corresponding differential quantities, e.g., stopping power, relative to water is possible (CT)

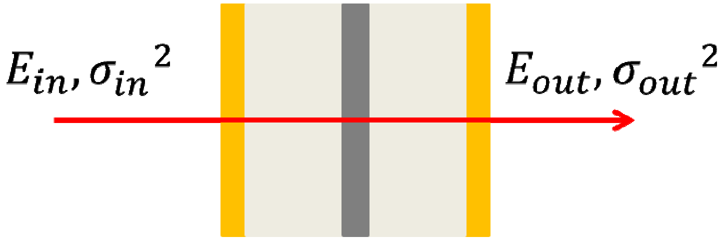

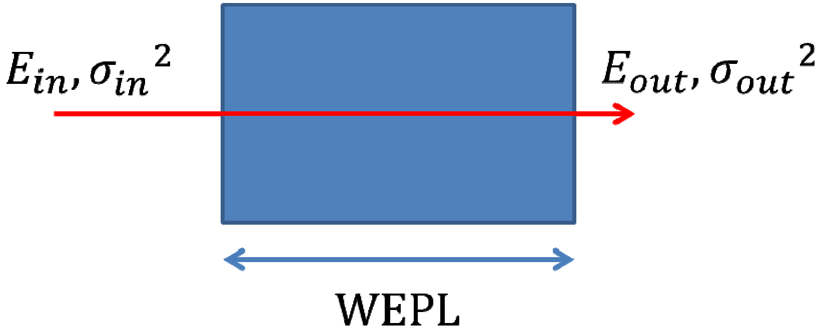

A SHORT HISTORY OF CHARGED PARTICLE RADIOGRAPHY AND CT

History of Proton Radiography (pRG)

- A. Koehler was the first to point out the potential value of pRG and to perform experiments with 160 MeV (Koehler, Science 160, 303–304, 1968)
- The higher density resolution but poorer spatial resolution than with x-ray radiography was noted by Koehler and later by Kramer et al. (Radiology, 1980)
- Medical interest in pRG as a QA tool for proton therapy was revived by U. Schneider and E. Pedroni at PSA during the 1990s
- pRG has been explored material testing at Los Alamos NL
- pRG continues to be explored for clinical use at MGH (J Seco, this meeting) and PSI
- More recently heavy ion radiography is being explored at the Heidelberg Ion Beam Therapy Center (K Parodi, this meeting)

Andy Koehler, former director of the Harvard Cyclotron)

Proton Radiography as a Tool to measure Range Uncertainties

Range Uncertainties

(measured with PTR)

> 5 mm

> 10 mm

> 15 mm

Schneider U. & Pedroni E. (1995), "Proton radiography as a tool for quality control in proton therapy," Med Phys. 22, 353.

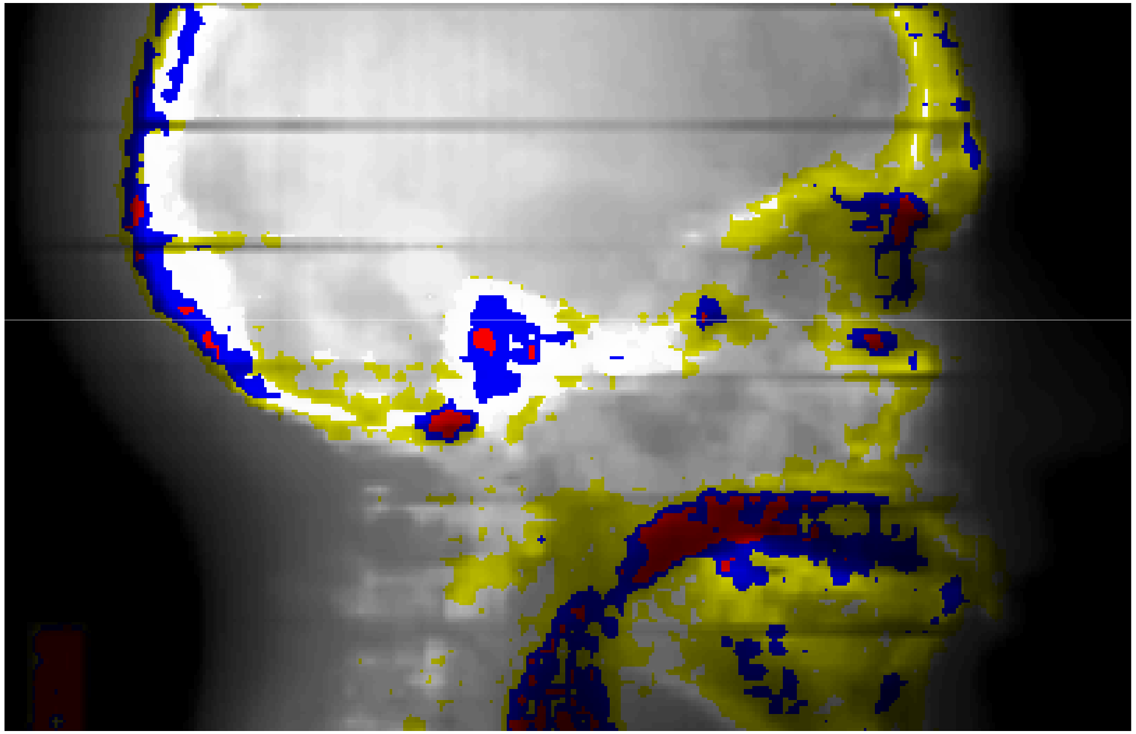

Alderson Head Phantom

History of Proton CT

- pCT is conceptually similar to pRG but consists of multiple pRG projections covering 360 deg followed by 3D image reconstruction
- Proton CT was originally suggested by A. Cormack in 1963
- First experiments were performed at LBL and LANL during the 1970s, and in Japan during the 1980s
- Clinical proton CT as a low-dose tomographic imaging modality was explored by R. Martin at Argonne NL during the 1990s
- A first pCT system was built by P. Zygmanski at the Harvard Cyclotron Lab in the late 1990s
- A pCT collaboration between researchers interested in pCT was formed at BNL in 2003
- pCT projects now exist at LLU/UCSC/CSUSB, NIU and FNAL, at INFN and IPHC

Particle CT in the 1970s

- Heavy ion tomography at LBNL 1972 – 1980 was explored by Cornelius Tobias and colleagues
- Proton computed tomography was investigated at LANL by Ken Hanson et al.

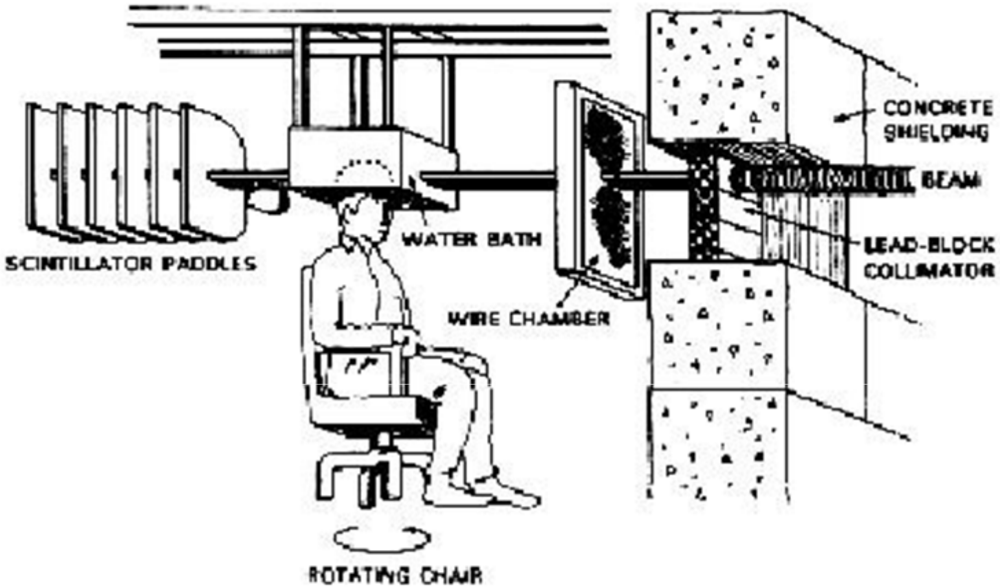

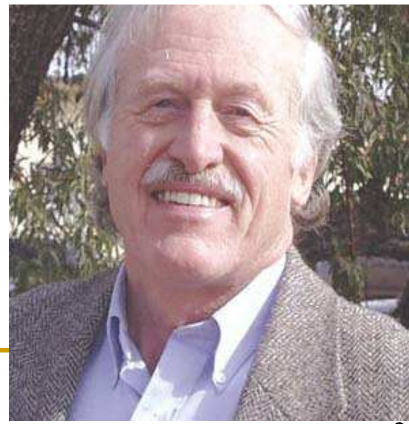

The Proton CT Collaboration

- A group of individuals with interest in proton imaging first met at BNL in Jan 2003 and LLUMC in Feb 2003 to develop a conceptual design for a modern pCT scanner based on single proton registration
- 2003 – 2007: Conceptual design, Geant4 simulations, most likely path concept, small prototype experiments
- 2008 – 2010: Phase 1 scanner for proof of principle
- 20011 – 2013: Phase 2 scanner for preclinical testing

Proton CT Scanner: Design Principle

- Protons of sufficient energy can penetrate the human body
- Protons can be tracked on the entry and exit side using modern Si detectors
- Residual energy detector to measure energy loss of individual protons
- Rotational detector arrangement in synchrony with proton gantry

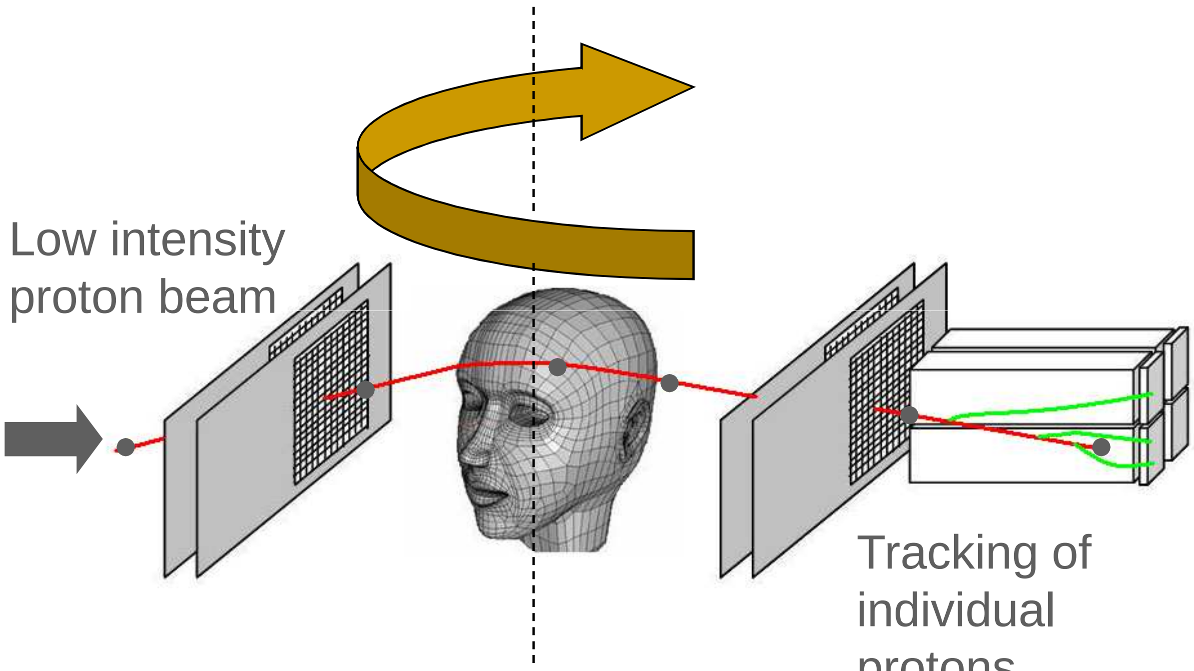

Design of a Proton CT Scanner rotating with the proton gantry

Proton CT with Single Particle Detection – Phase 1 Scanner

- First concepts were derived from proton radiography systems developed at PSI
- Fully developed concept of pCT (IEEE NSS/MIC 2003)
- This pCT concept is realized in the Phase 1 scanner

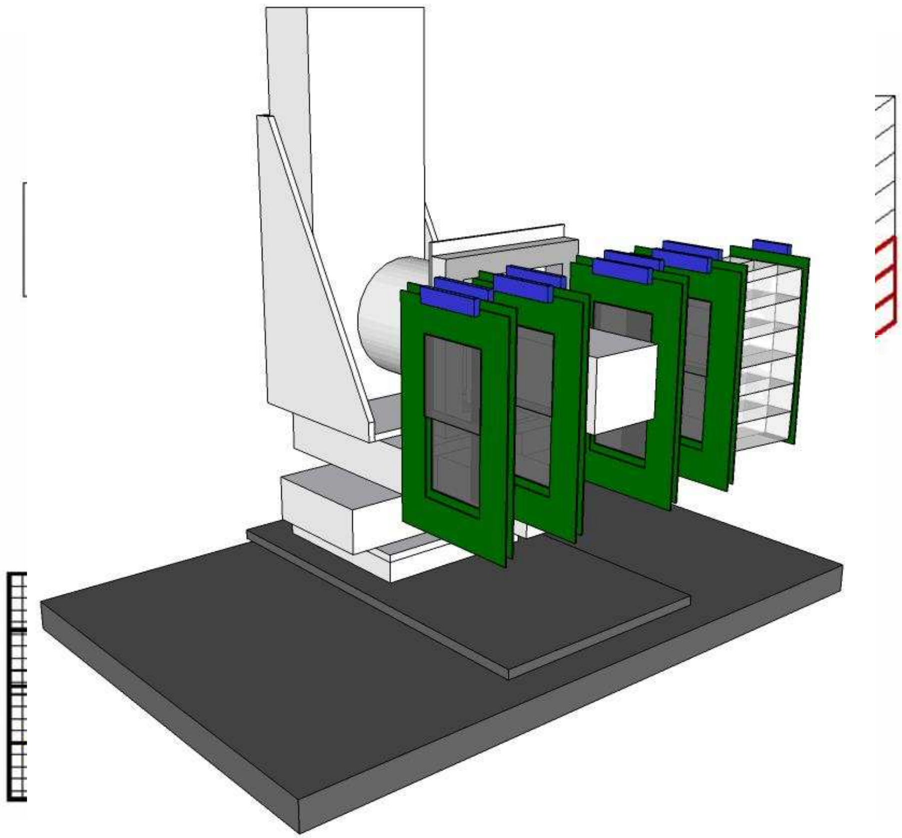

Single Particle Concept: Advantages and Challenges

- Single particle detection allows for
  - rejection of unsuitable events (“data cuts”)
  - estimation of individual proton paths
  - use of iterative reconstruction algorithms based on single proton histories
- Challenges of single particle detection
  - Requires high data rates (fast DAQ systems)
  - Requires computation tools exploiting sparsity and massive parallelism

Summary of pCT Design Principles

- Detect location of individual primary particles, reject non-related events (e.g., cosmic rays, noise) or unsuitable events (e.g., large-angle scattering, inelastic nuclear interactions)
- Reconstruct charged particle path as accurately as possible
- Measure residual energy or range of charged particle as accurately as possible
- Convert residual energy/range to water-equivalent path length (WEPL)
- Define the pCT reconstruction problem for RSP using as much information as possible and apply efficient reconstruction algorithm (parallizable)
- Perform pCT reconstruction as efficiently as possible (GPU/CPU cluster)

Phase 1 pCT Tracker

- The Phase 1 pCT tracker consists of front and rear module for location and direction measurements
- Modules: two detector boards measuring the X-Y position in two locations => direction
- Detector boards: 4 Si Strip Detectors (SSDs), 9 cm x 9 cm, 384 strips, 0.23 mm pitch
- Strips of one SSD oriented in either vertical or horizontal direction (X and Y sensitivity)
- Total sensitive area 9 cm x 18 cm
- Modified GLAST/Fermi readout chip, max rate 200 kHz

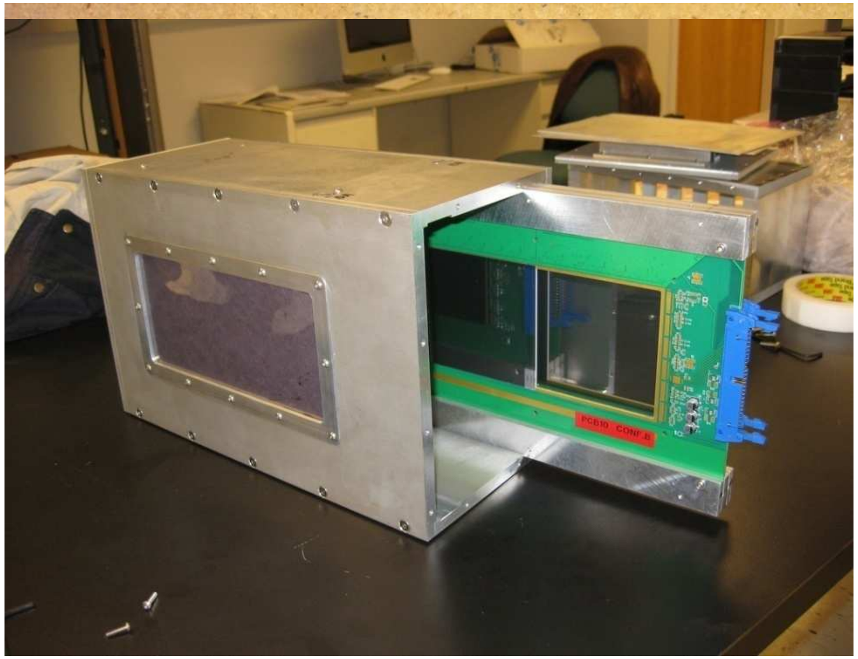

Detector board with 2 SSDs in the front (visible) and 2 SSDs in the back of the board

Phase I pCT scanner front module

Silicon Tracker Improvements

- Large-area coverage requires tiling of Si sensors
- Largest available sensors are ~9 cm x 9 cm single-sided Si strip detectors cut from 6 inch wafers (Hamamatsu)
- Strip pitch 0.23 mm
- These sensors, in their native form have ~1mm inactive edges which will create image artifacts (see next slide for solution)

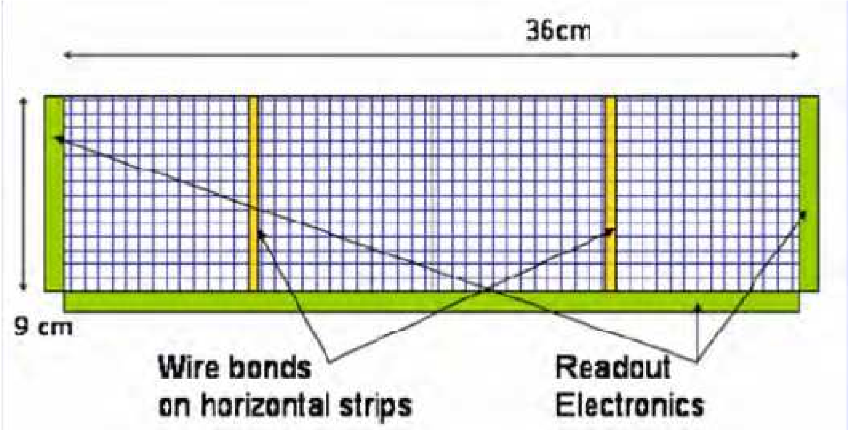

Layout of one of the four x-y tracker planes using 9 cm x 9 cm single-sided silicon detectors with one side rotated by 90 degrees.

Novel Si Sensors with "Slim" Edges

Courtesy Hartmut F-W Sadrozinski, UCSC

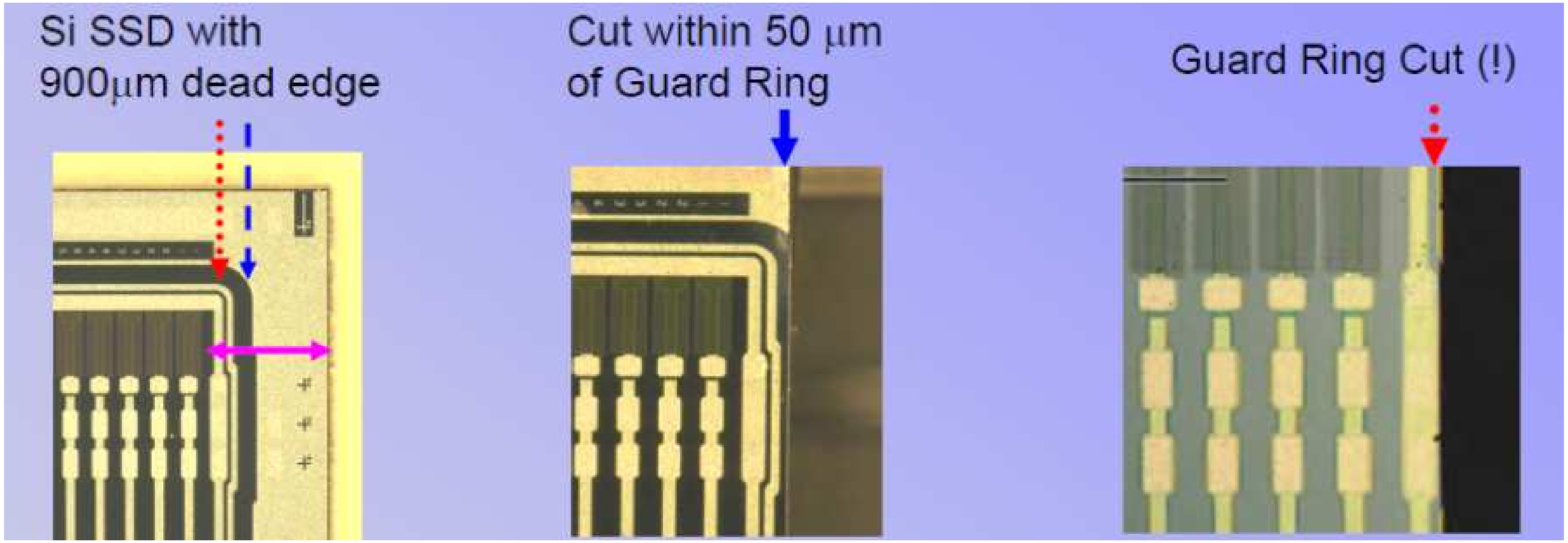

- The corner of a sensor manufactured by Hamamatsu Photonics for the GLAST mission is shown on the left with the planned cut indicated by the red line
- The sensor was etch-scribed with XeF2, cleaved and passivated with nitrogen plasma-enhanced chemical vapor deposition (PECVD)
- The slim edge with strips and bias ring is shown on the right; only traces of the guard ring are visible.

Next Generation pCT Tracker/ASIC

- 4 (x/y) SSDs (9 cm x 9 cm) per tracking layer cut from 6” high-resistivity n-intrinsic silicon wafers
- Eight layers of silicon strip detectors are read out by 144 64-channel ICs, each with a 100 Mbit/s link to an FPGA on the same board
- Nominal data rate ~10^6 protons per sec

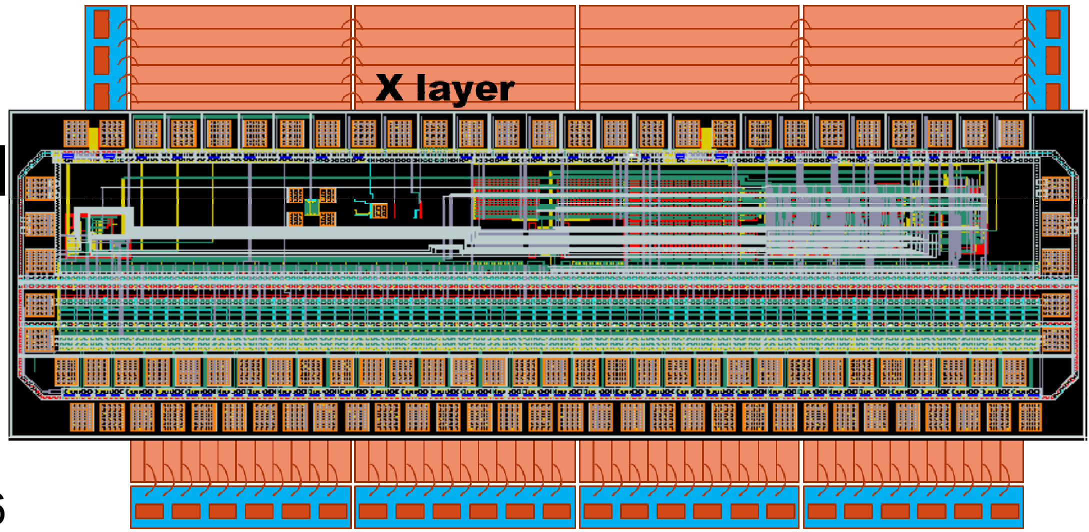

Next Generation pCT Data Readout/Data Flow

- Readout is triggered by energy/range detector and tracker
- Buffering at front end to minimize dead time
- Eight layers of SSDs read out by 144 ASICs and linked to an FPGA (Spartan 6, Xilinx)

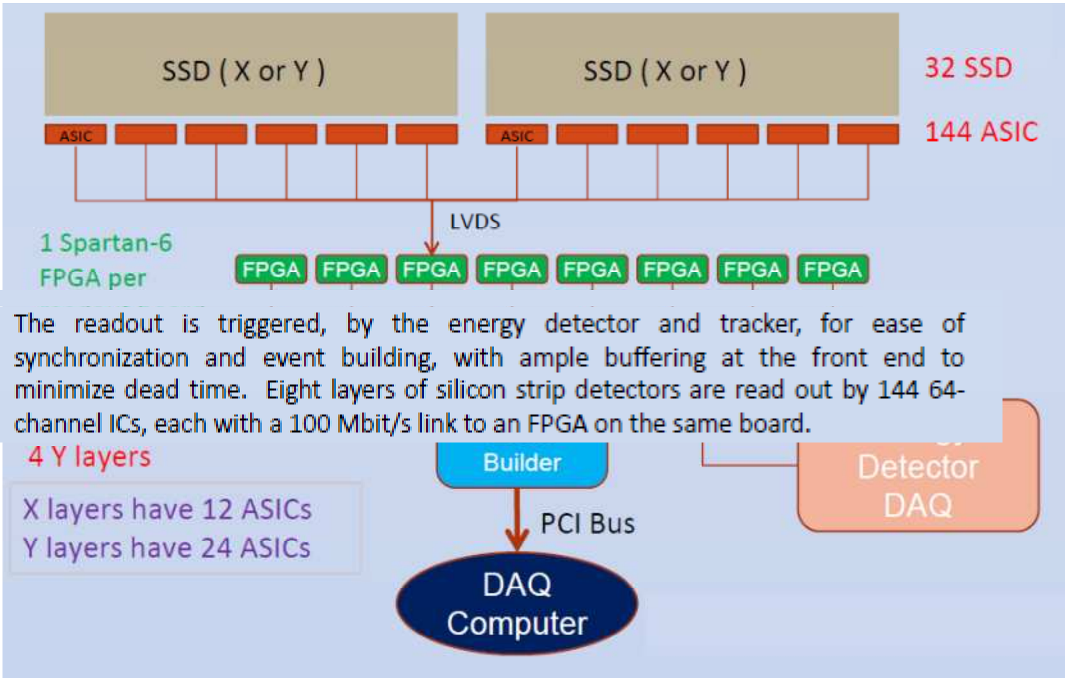

Phase 1 Energy Detector: Crystal Calorimeter

- Crystal matrix with 18 thallium-doped cesium-iodide (CsI(Tl)) crystals (~3.6 cm x 3.6 cm x 12.5 cm)
- Each crystal read out by area-matched Si photodiode
- Si photodiode => preamp/shaper => ADC
- Excellent linearity and energy resolution < 1% above 40 MeV
- Integrated with rear tracker module

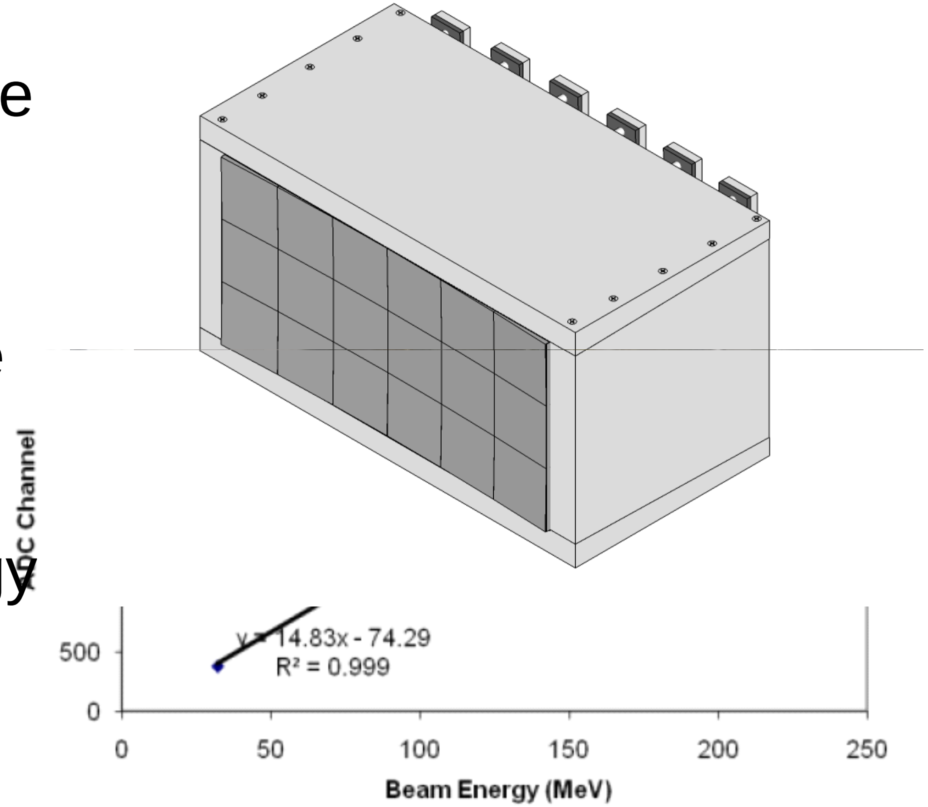

Calorimeter Calibration:
Individual Crystal Weighting

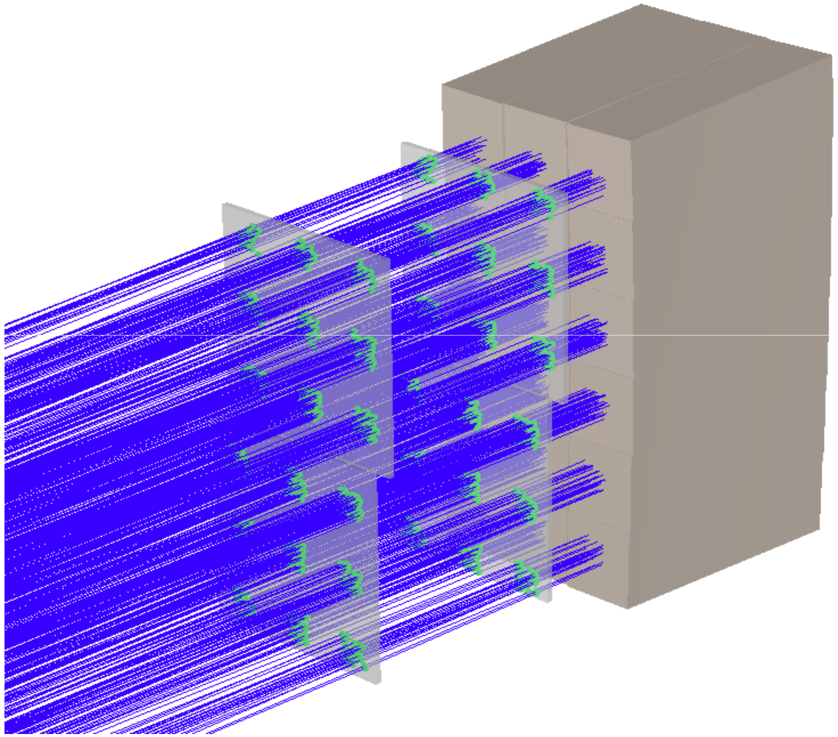

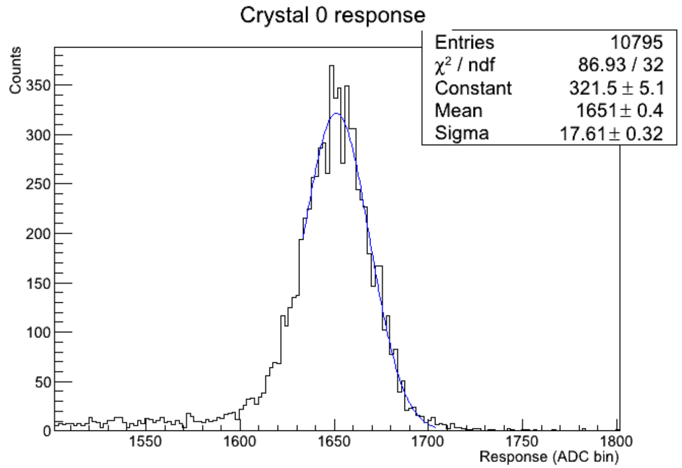

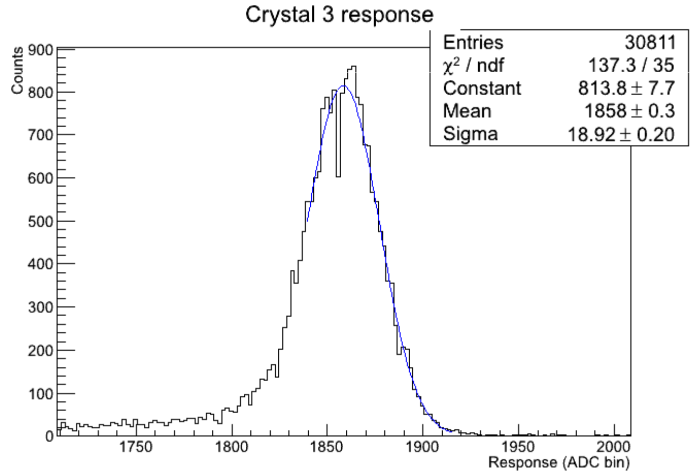

Individual responses are weighted and summed

Calorimeter Calibration:
WET Calibration

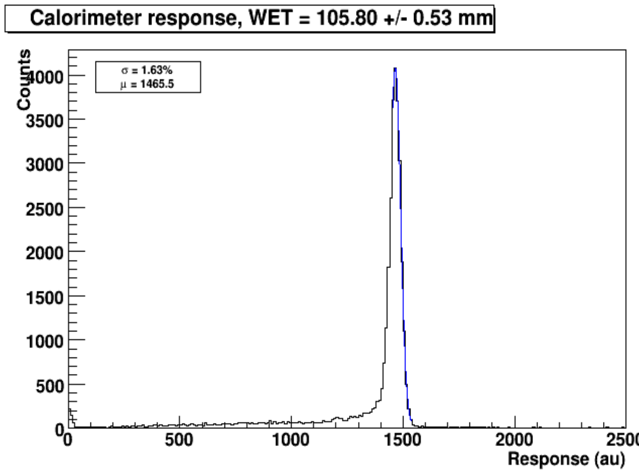

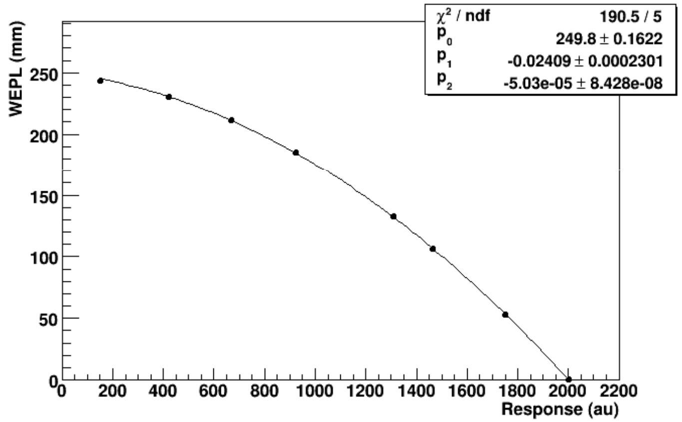

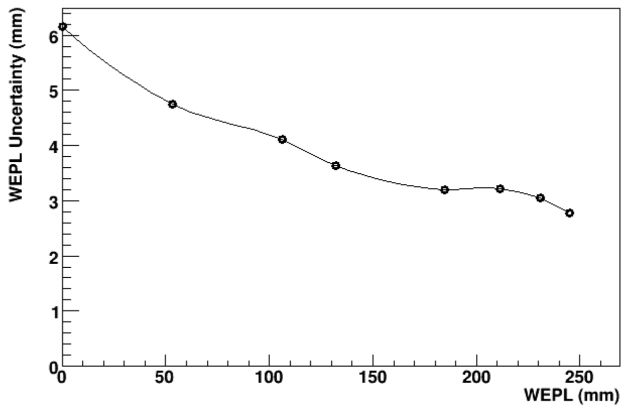

- Polystyrene blocks of known thickness and RSP
- Produces a second order polynomial, providing fast conversion from detector response to WEPL
- Procedure takes 15 minutes and can be performed daily

Calorimeter Calibration:
WET Calibration Verification

Used WEPL calibration method to determine RSP of tissue equivalent materials from Gammex:

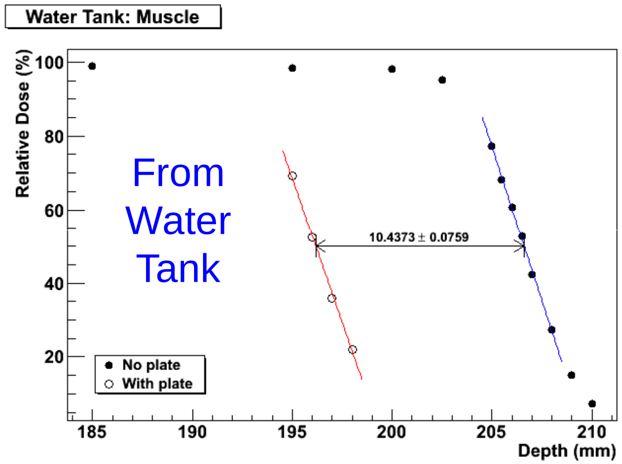

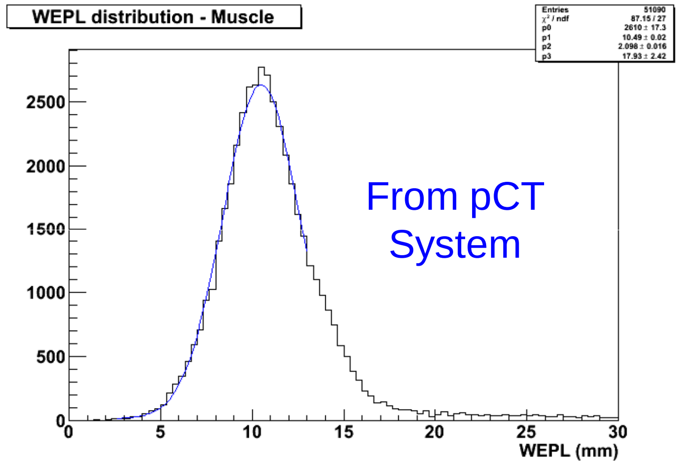

	Range Shift		pCT	
Material	RSP	σ_{RSP}	RSP	σ_{RSP}
Lung	0.267	0.005	0.268	0.001
Adipose	0.947	0.007	0.943	0.002
Muscle	1.032	0.008	1.037	0.002
Brain	1.062	0.007	1.064	0.002
Liver	1.076	0.005	1.078	0.002
Cortical Bone	1.599	0.007	1.595	0.002

Problems with Phase 1 Calorimeter

- Despite careful calibration, inhomogeneous response to proton histories of same residual energy (WEPL) could not be resolved
- Analysis revealed that this complicated response is due to light leakage at the level of the PDs and jitter of the timing of different front end chips

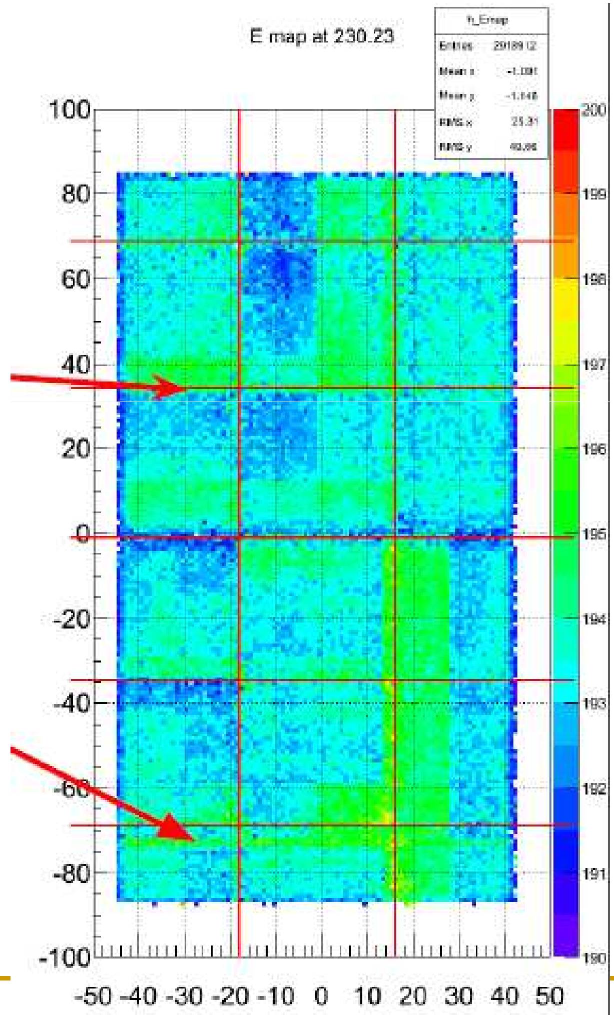

System Alignment:
Tracker Offsets

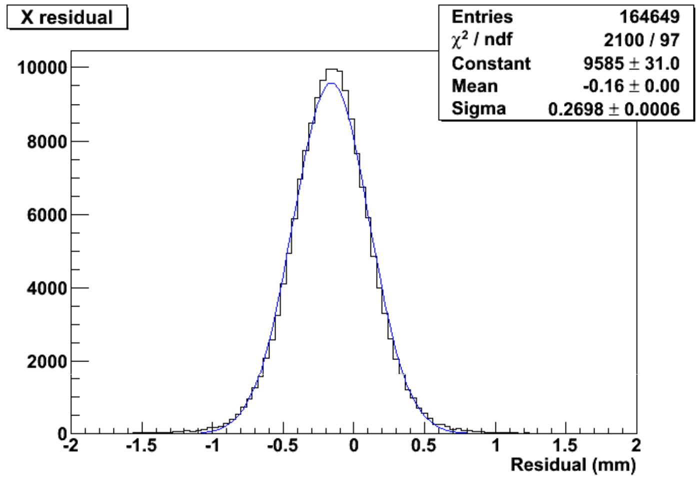

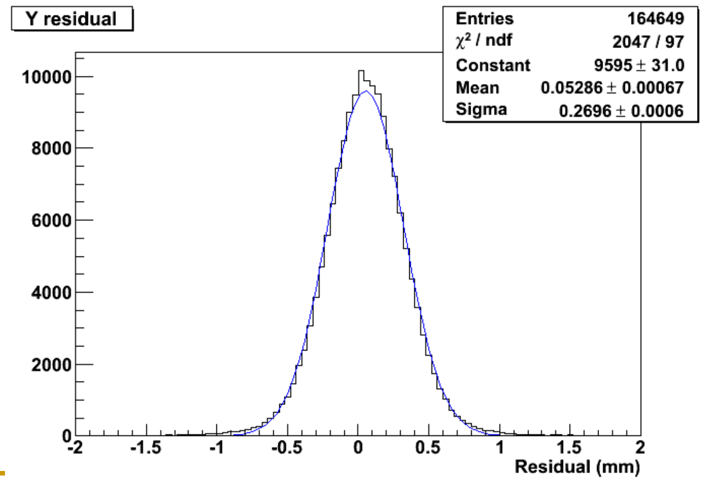

Use straight tracks from beam to calculate x and y corrections

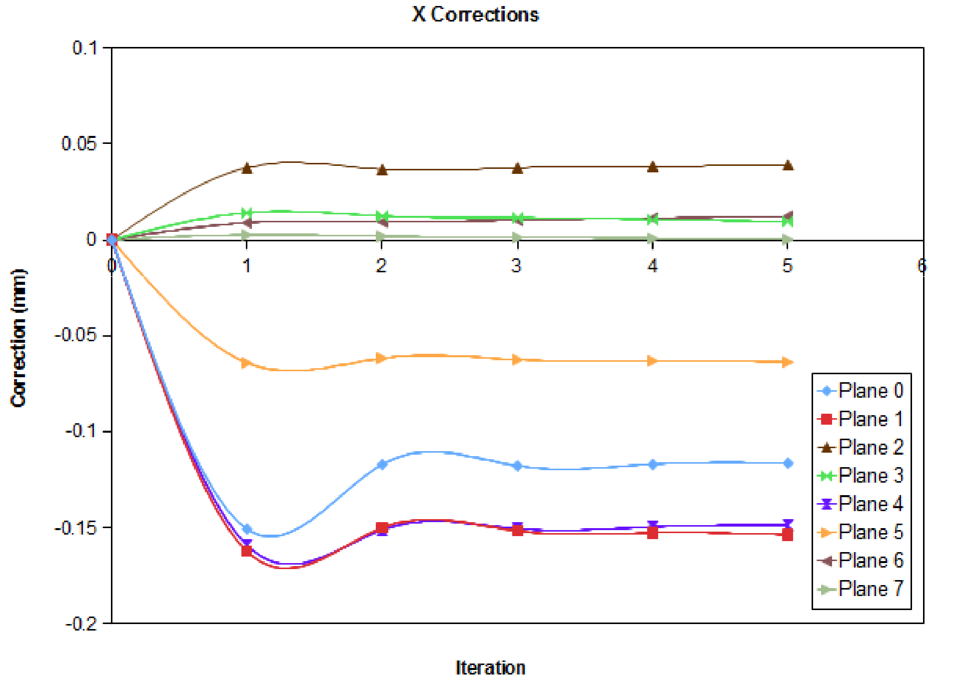

Requires 1 minute of beam data without the phantom, performed daily.

System Alignment:
Rotational Axis Definition

- Rotation axis position must be defined relative to the detector coordinate space.
- Location along the beam axis (*z*) is defined mechanically.
- Vertical location (*y*) is determined by imaging a plastic rod mounted off axis:
  1. Projection data are recorded at various angles.
  2. Center of rod is found in “sinogram,” for each projection angle.
  3. Constant from sine wave fit corresponds to vertical misalignment of axis

  → Correct for this in software

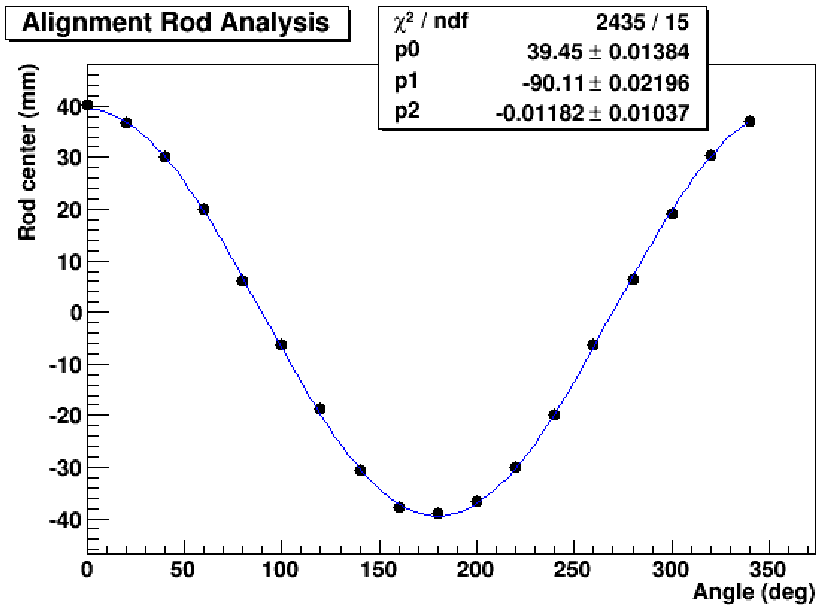

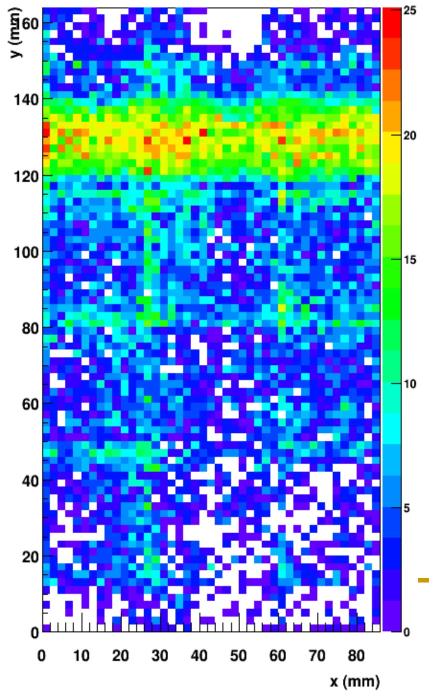

This procedure takes 20 minutes and is performed periodically (~monthly).

Next Generation pCT Energy Detector

- A multi-stage scintillator (MSS) registers energy response; the response of the stopping scintillator is converted to WEPL
- The WEPL resolution is high (~3 mm), combined with good light yield and uniformity
- MSS design is preferred compared to stack of multiple thin scintillators (range counter) based on cost considerations

R3318 PMT

Phase I pCT Scanner at LLU (completed in 2010)

- System component integration & mounting (April 2010)
- Tested initially with radioactive source and cosmic rays (muons)
- Installation on proton research beam line & 1st test runs (May 2010)
- Spill uniformity optimization (June 2010)
- Scanner calibration (July 2010)
- Experience collected with phantom scans since Dec 2010, leading to Phase 2 pCT scanner

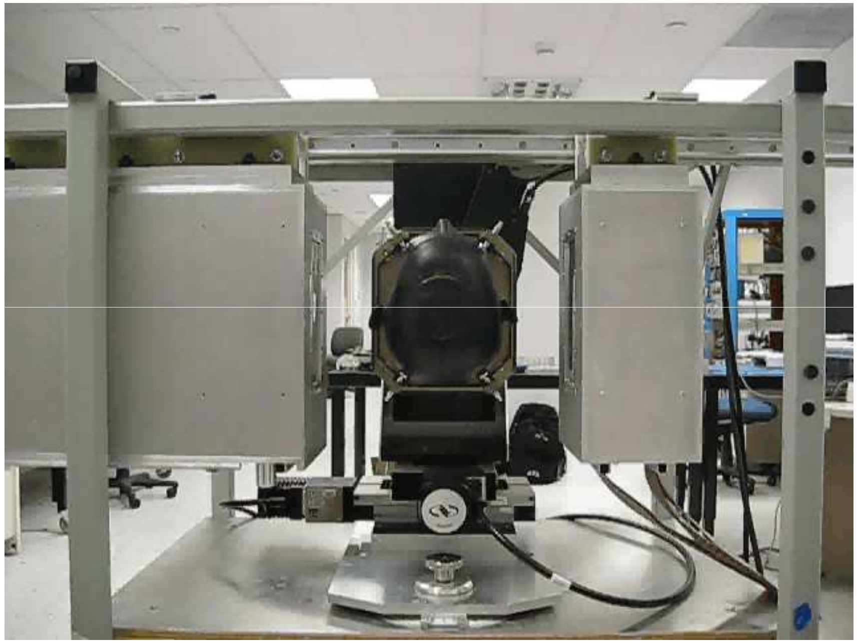

PCT trigger diagram

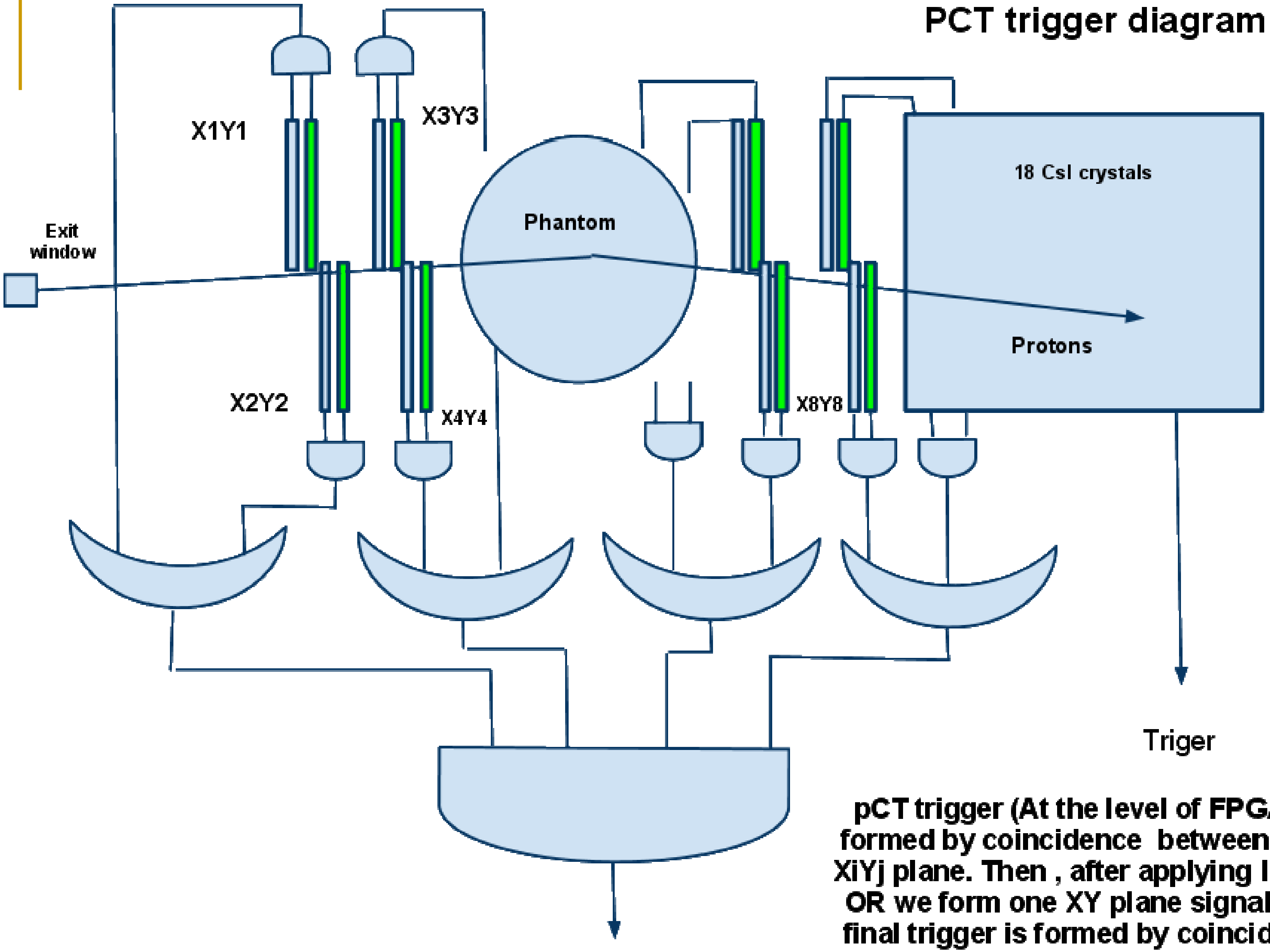

pCT trigger (At the level of FPGA) is formed by coincidence between each XiYj plane. Then , after applying logical OR we form one XY plane signal. The final trigger is formed by coincidence of 4 XY planes or by calorimeter signal.

Data Flow Chart (Tracker, 1 of 16)

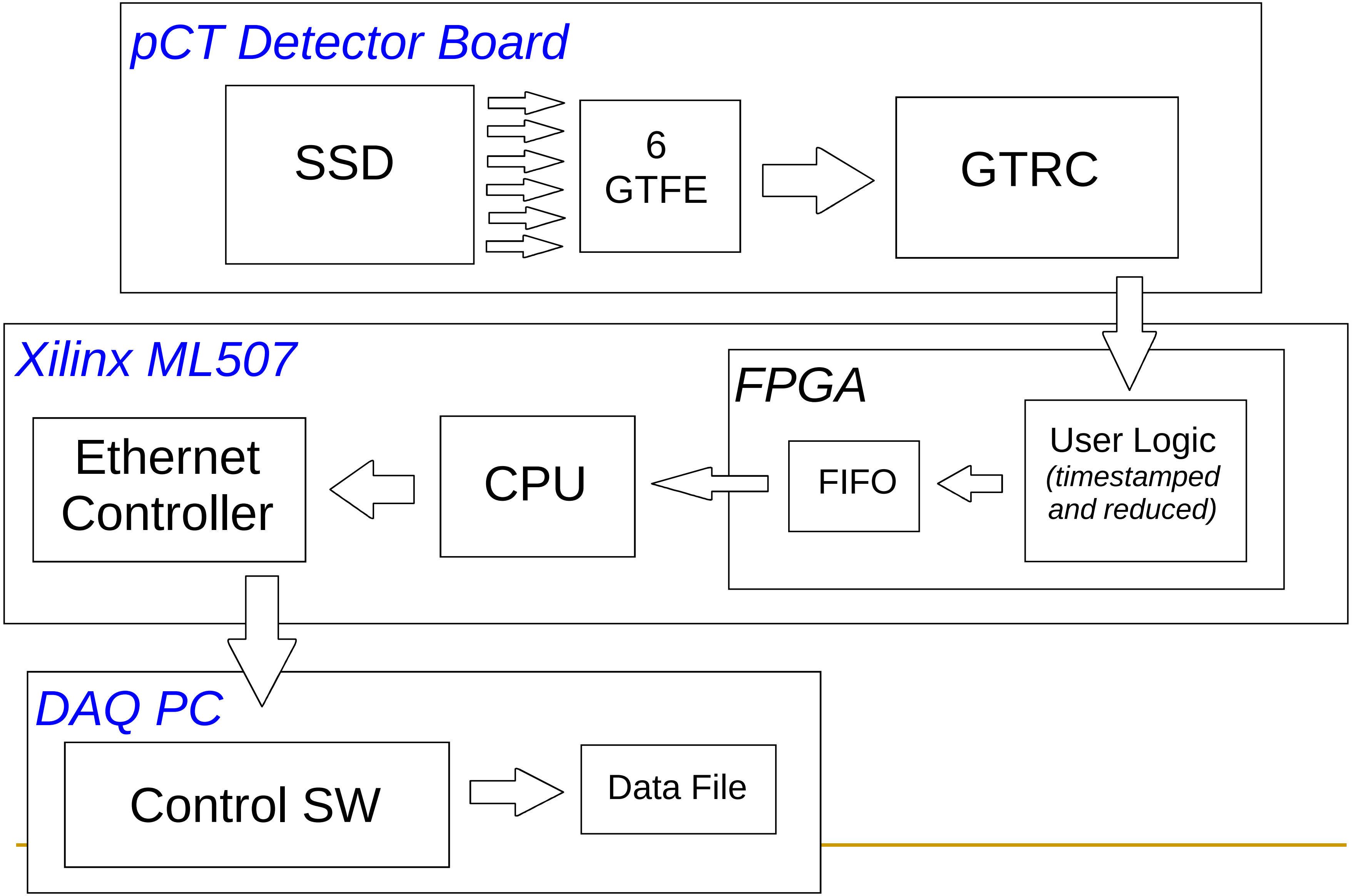

DAQ Software

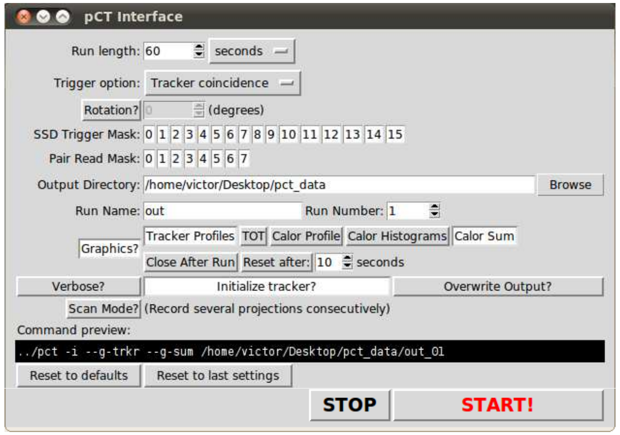

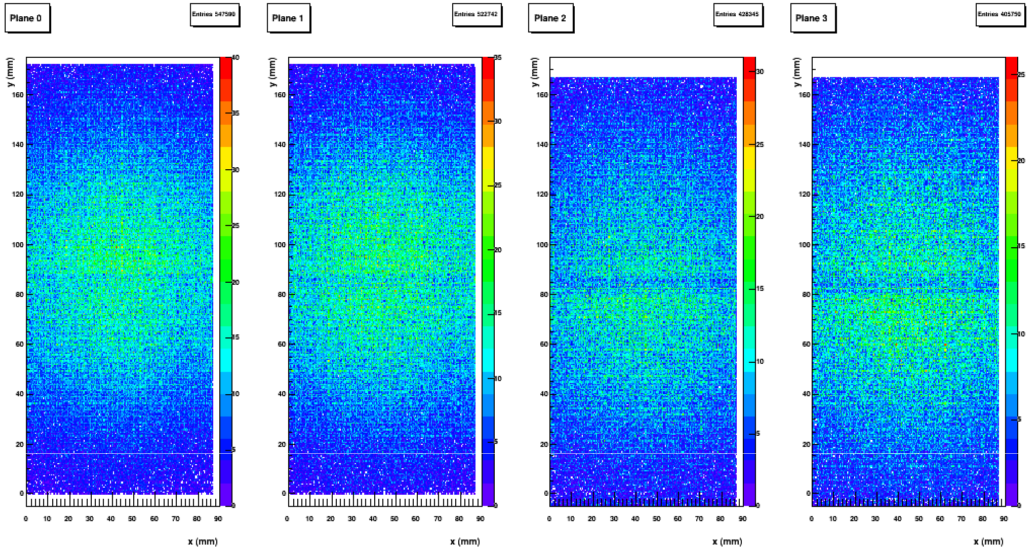

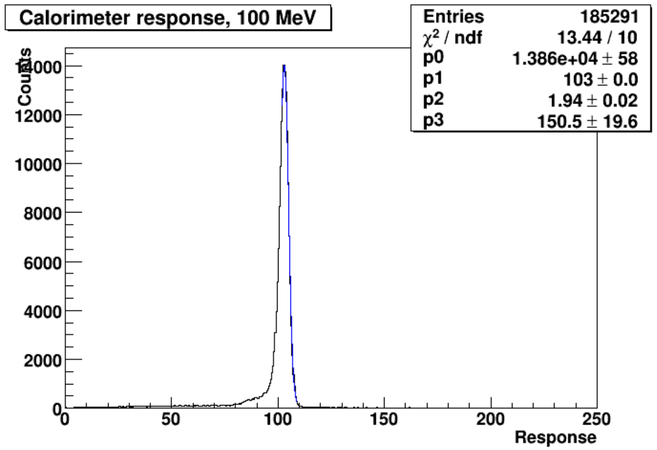

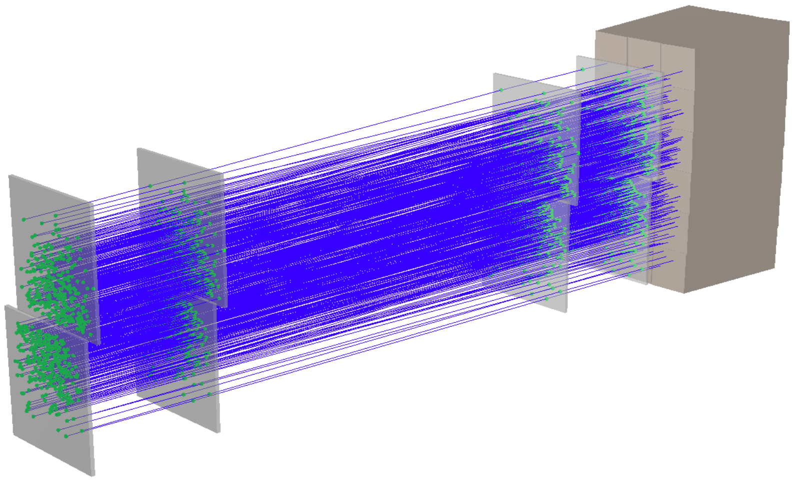

The Phase 2 pCT Scanner (Summer 2013)

- Large area tracker suitable for head scans + immobilization devices (36 cm x 9 cm
- Multi (5)-stage scintillation detector calibrated for WEPL measurements
- Vertical axis rotation stage for phantom rotation on fixed horizontal beam line
- FPGA-based readout and reconstruction on GPGPU cluster
- Currently, transition from Phase 1 to Phase 2 (Phase 1.5)

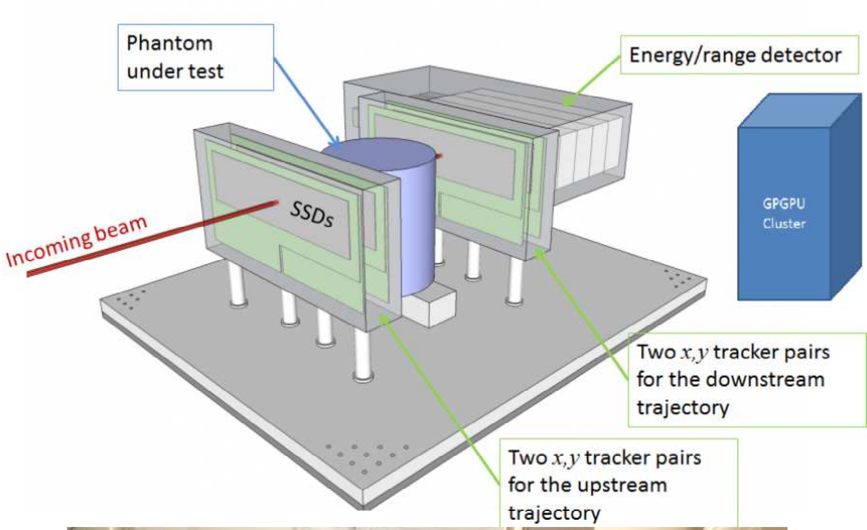

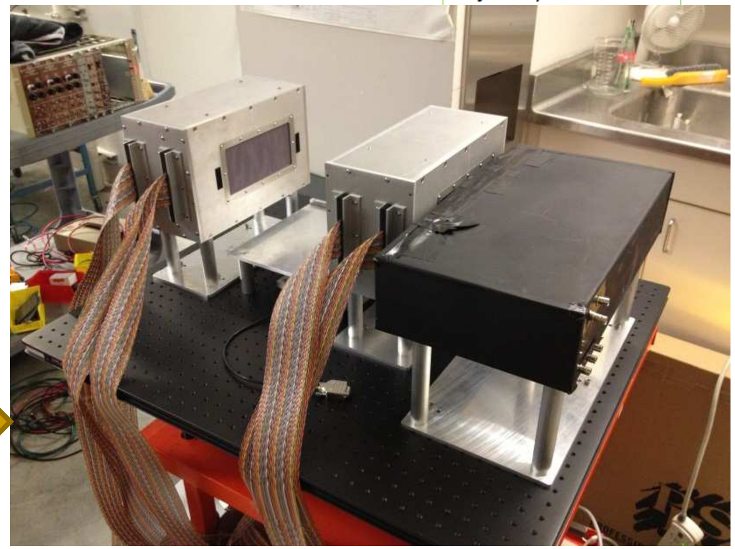

pCT RECONSTRUCTION AND PHANTOM SCANS

Linear pCT System and Solution Concept

- Linear System
  - i =1…m measurements => vector b = (b_i)
  - Object vector x = (x_j), j=1…n
  - Projection matrix A = (a_{ij})
- Note: matrix A is very large & sparse, and the system is inconsistent
- Find "adequate" solution of Ax=b using iterative projection method (projection onto hyperplanes H_i)
- Parallel algorithms for pCT have been developed over the last 5 years by Penfold, Censor & Schulte

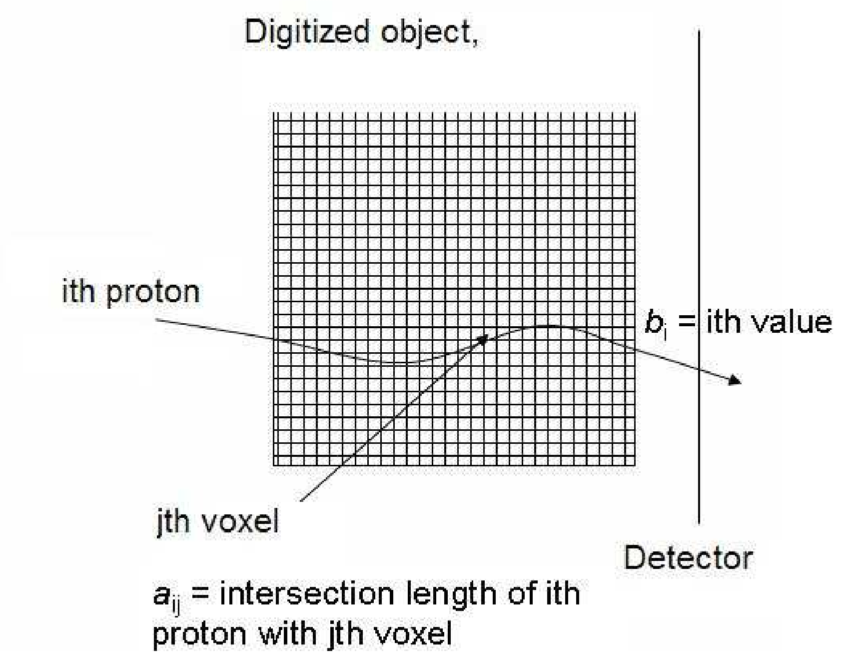

$$H_i = \{x \in \Re^n \mid \langle a^i, x \rangle = b_i, \text{ for } i = 1, 2, \ldots, m.$$

Path Reconstruction Concepts

- Different proton paths may be used in the reconstruction: MLP = Most Likely Path, SLP = straight line path, CSP = cubic spline path
- The MLP is determined by maximizing likelihood (chi square) of output parameters, given entry parameters
- MLP significantly improves spatial resolution compared to SLP, CSP reconstruction is nearly as good as MLP reconstruction as shown by Li & Schulte (Med Phys 2006) and later by Wang et al. (PMB 2011)
- The MLP concept was formulated by Williams (PMB 2004), & further refined by Schulte et al. (Med Phys 2008)

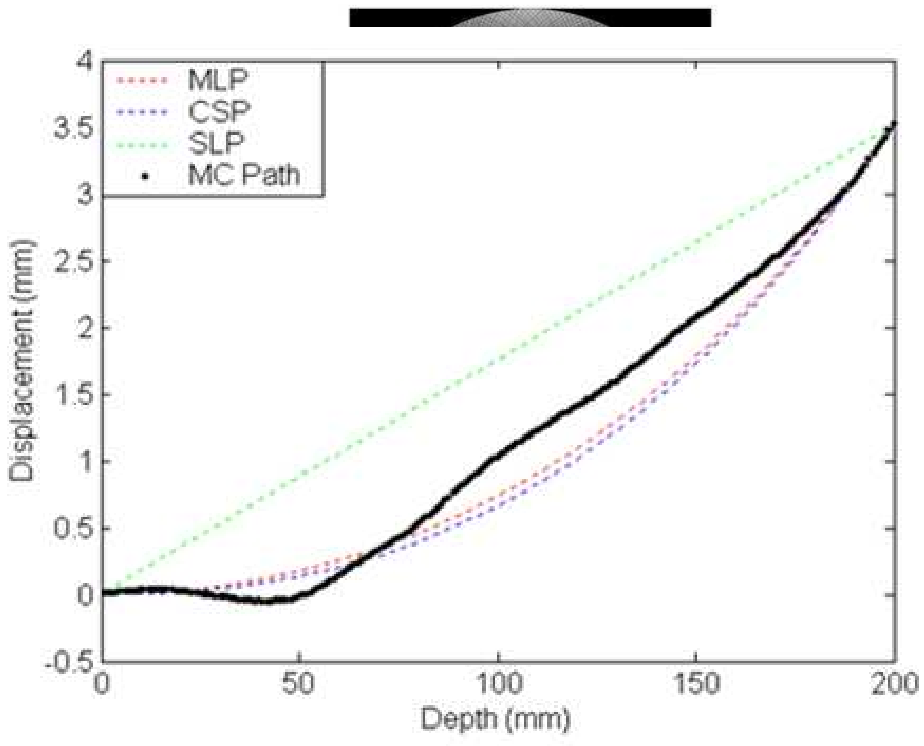

The Mathematics of Iterative pCT Reconstruction

- Linear System
  - i =1…m measurements => vector b = (b_i)
  - Object vector x = (x_j), j=1…n
  - Projection matrix A = (a_{ij})
- Note: matrix A is very large & sparse, and the system is inconsistent due to noise in b (energy measurement) *and* A (path uncertainty)
- Find "adequate" solution of Ax=b using iterative projection method (projection onto hyperplanes H_i)

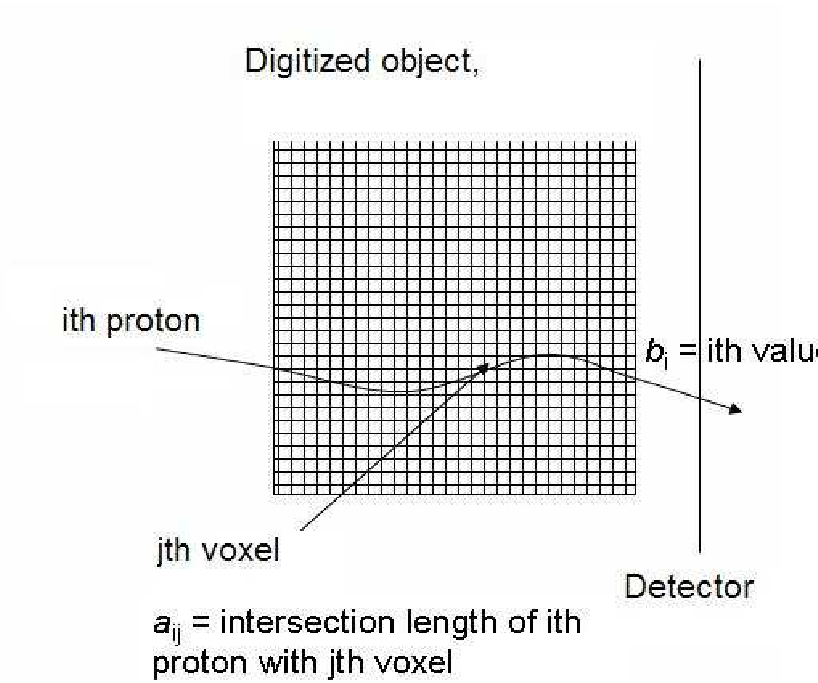

$$H_i = \{x \in \Re^n \mid \langle a^i, x \rangle = b_i, \text{ for } i = 1, 2, \ldots, m.$$

First pCT Scanning Results with the LLU/UCSC/NIU pCT Scanner

- A series of pCT scans of a polystyrene Lucy phantom with cylindrical air, acrylic, and bone-equivalent plastic cavities/inserts were done after completion and first calibration of the Phase 1 pCT scanner
- Reconstructions with an iterative algorithm (DROP-TVS) were performed on an NVIDIA GPU

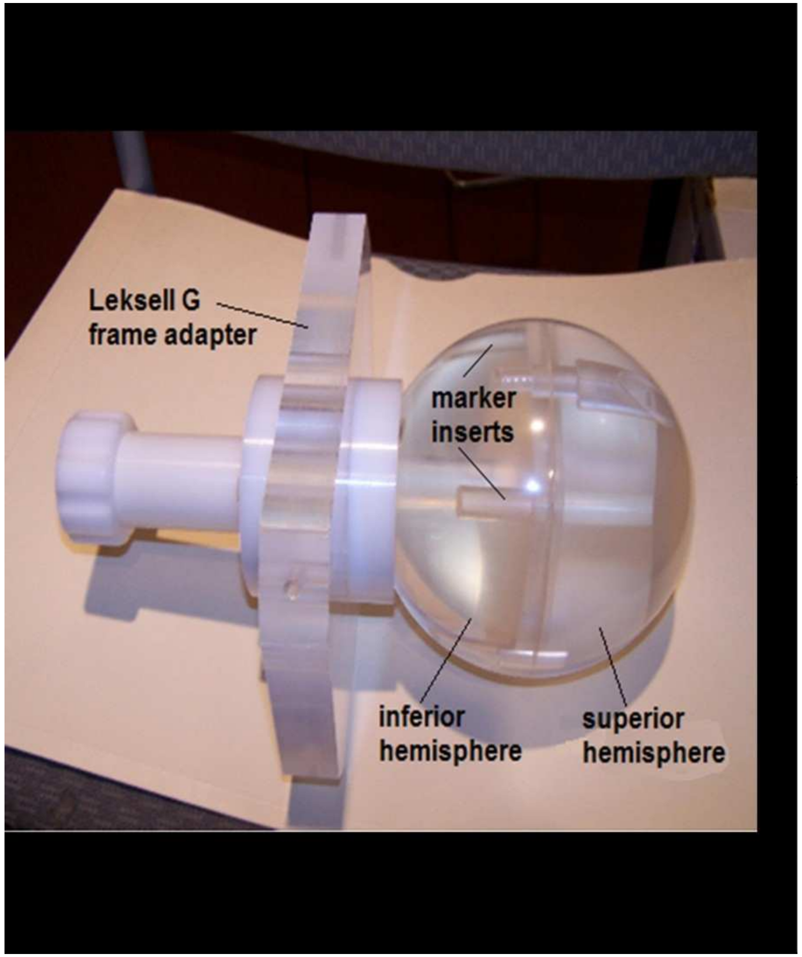

pCT Reconstruction: A Linear Convex Feasibility Problem

- Ideal case: proton energy measurements are noise-free, and MLP's are exact -> all hyperplanes intersect in one point corresponding to the true object function
- Real case: proton energy measurements are **not** noise-free, and MLPs are **not** exact -> hyperslabs may intersect in a convex region containing the true object function

$$S_i = \{x \in \mathbb{R}^n \mid g_i(x) \le 0\} \text{ find } S = \bigcap_{i=1}^{m} S_i$$

in our case

$$g_i(x) = \left| \langle a^i, x \rangle - b_i \right| = 0$$

$$g_i(x) = \left| \langle a^i, x \rangle - b_i \right| - \varepsilon_i \le 0$$

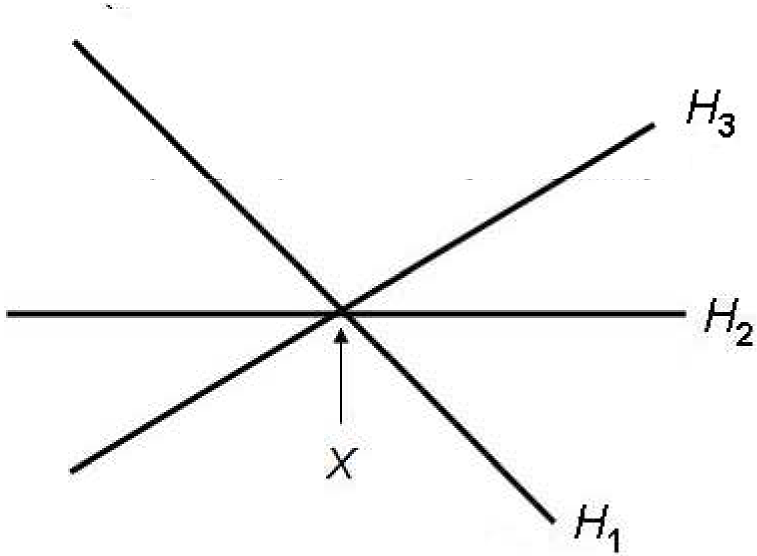

Projection Methods – The Classics

- Fully sequential: ART (Kaczmarz, 1937)
  - standard, used in many applications
  - Proven to work in pCT
  - Slow due to sequential nature
  - Can be made parallel in principle
- Fully simultaneous (Cimmino, 1937)
  - Converges to least-squares minimum
  - Very slow due to small weight (1/m)

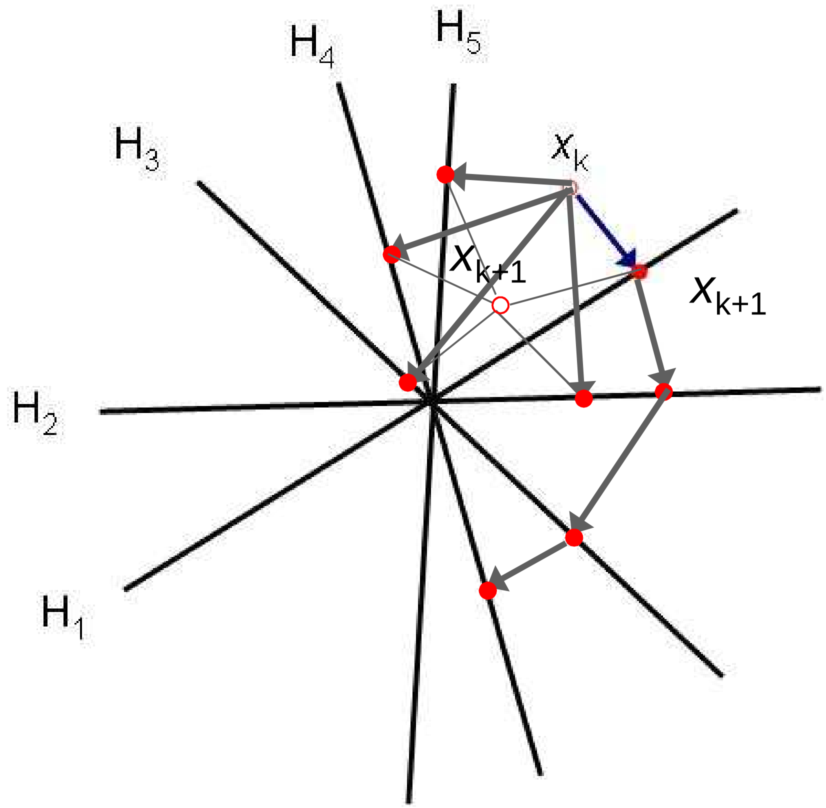

Projection Methods – Block-Iterative and String-Averaging Methods

- Block-Iterative Projection (BIP) (Aharoni & Censor 1989)
  - Simultaneous projection within blocks of hyperplanes
  - Sequential projection of block iterates
  - Weighting according to block size (avoiding small 1/m)
- String-Averaging Algorithm (Censor, Elfving, Herman, 2001)
  - Sequential projection within strings of hyperplanes. in parallel within all strings
  - Convex combination of all string iterates

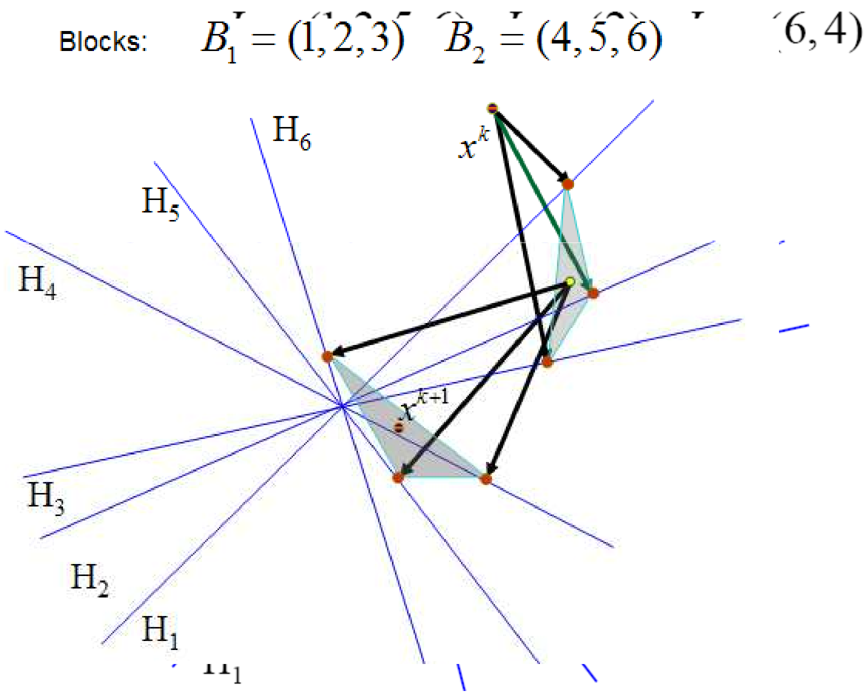

Total Variation Superiorization

- First suggested by Butnariu, Davidi, Herman, & Kazantsev, IEEE J. Sel. Top in Sign Proc, 1, 540–547 (2007)
- Under certain conditions, perturbation of the k-th image iterate leads to a “superior” image in terms of smaller total variation
- Easier to perform than optimization and better result than solving the feasibility problem without superiorization
- Has shown promising results in X-ray CT reconstruction

TVS-DROP Reconstruction Results

Circular phantom with central high-contrast feature (for MTF), bone shell, and brain interior – DROP/TVS has

- Less noise
- Better accuracy
- Better stability
- Improved spatial resolution
- Better contrast discrimination

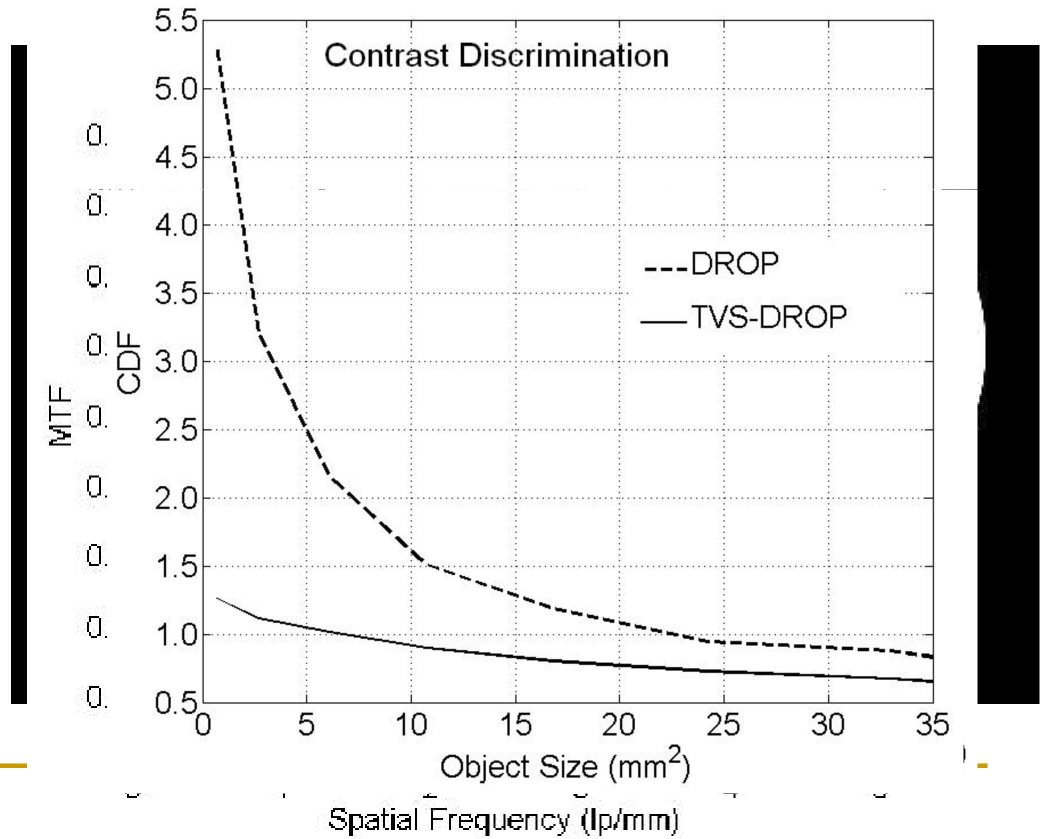

Complete Lucy Phantom Scan

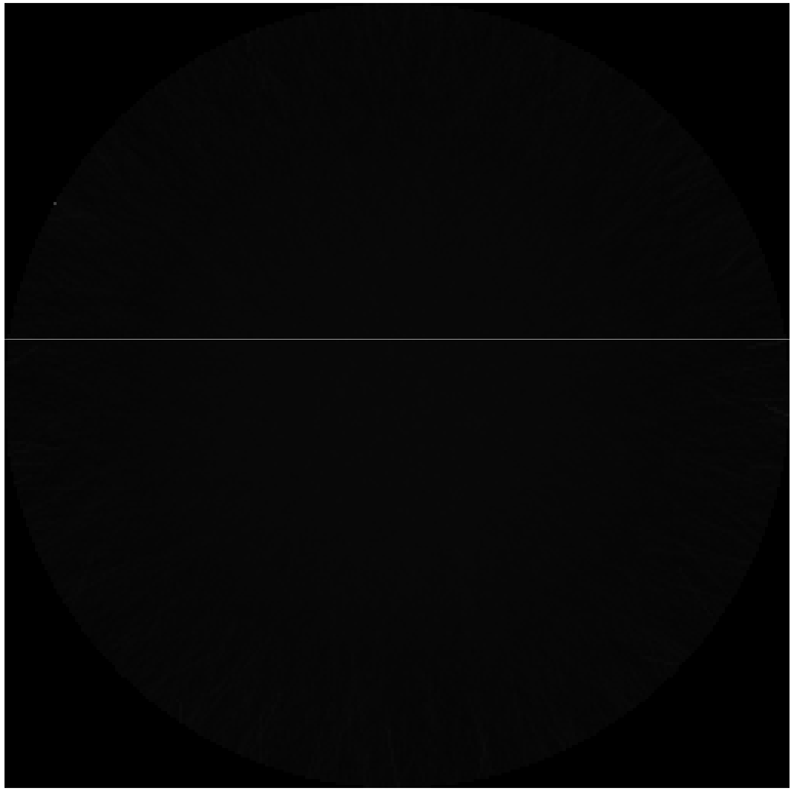

Water Phantom Scan

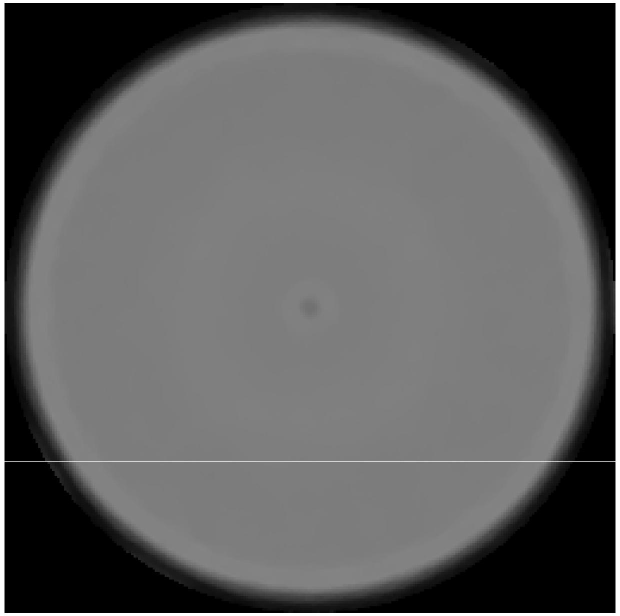

- 15 cm diameter acrylic cylinder filled with degassed water
- Reconstruction based on 4.3×10^7 proton histories
- Total scan time: ~6 hours
- 200 MeV beam energy
- 90 projections (4 degree steps)
- 16 x 16 x 8 cm^3 reconstruction volume
- 256 x 256 pixels, 32 slices
  → 2.1×10^6 voxels
- 0.625 x 0.625 mm pixel size
- 2.5 mm slice width

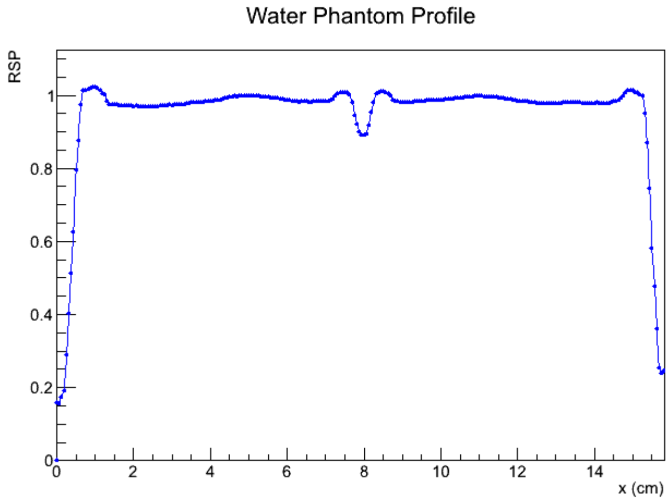

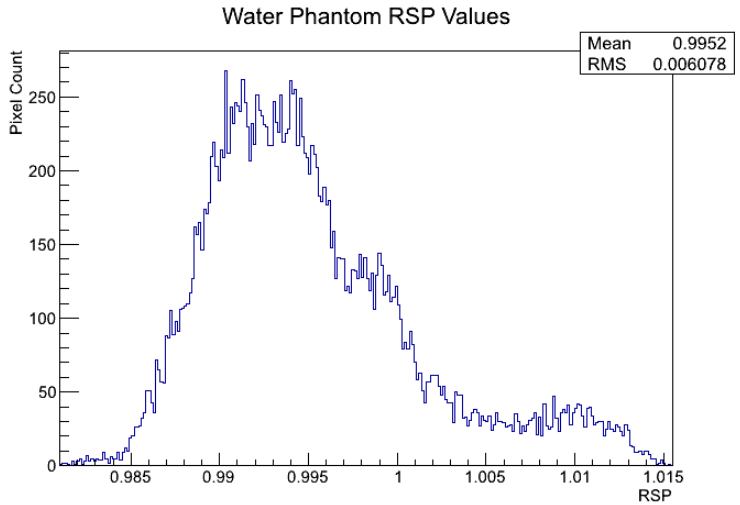

Head Phantom Scan

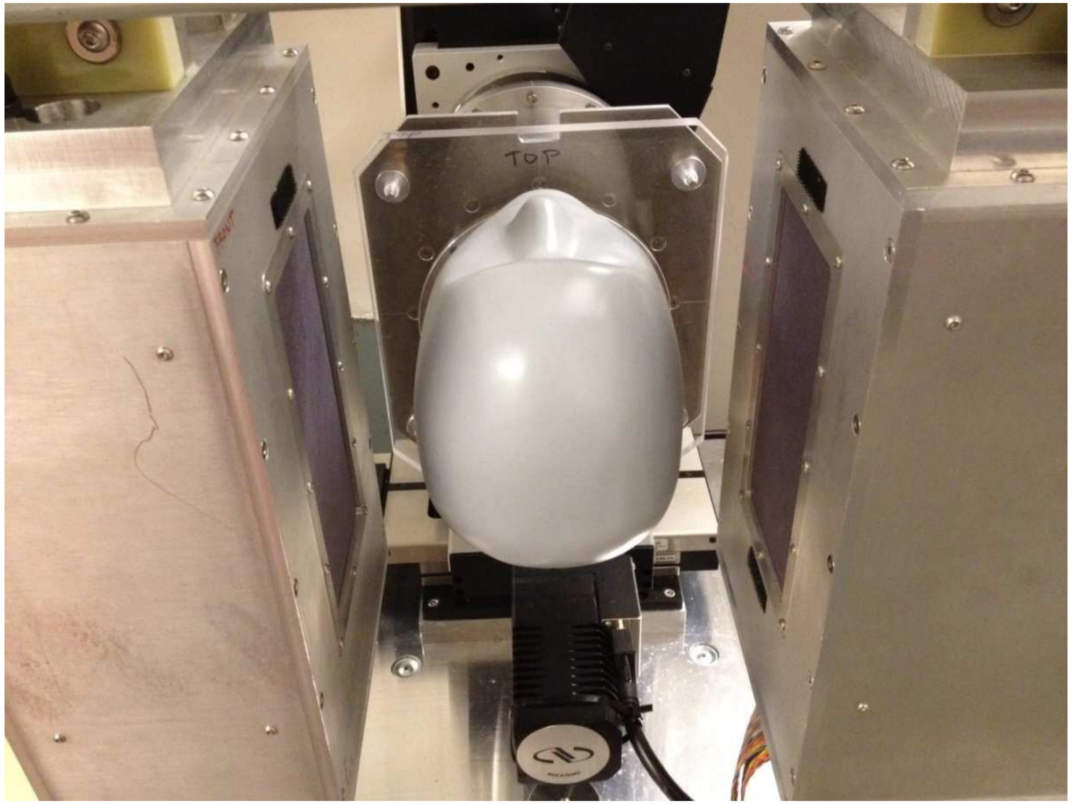

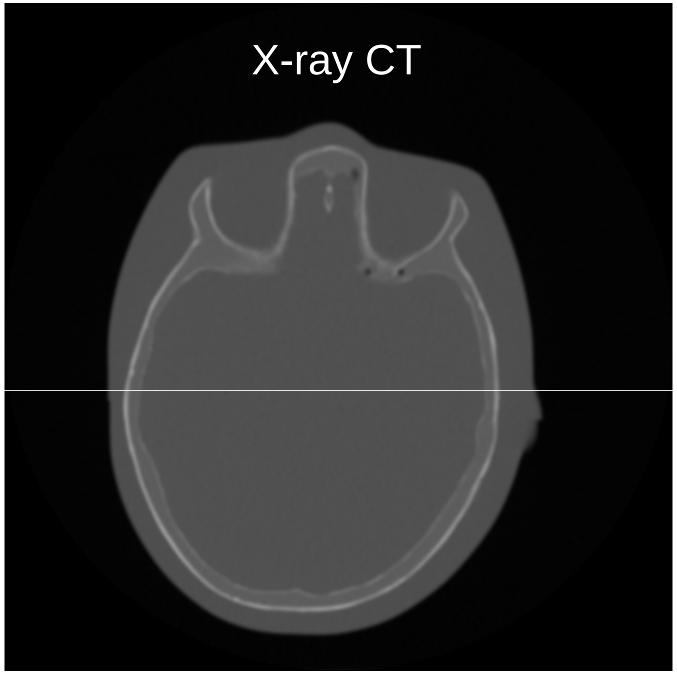

- CIRS HN-715 Pediatric head phantom
- Realistic head and neck geometry and densities
- 7 different tissue equivalent materials

Head Phantom Scan

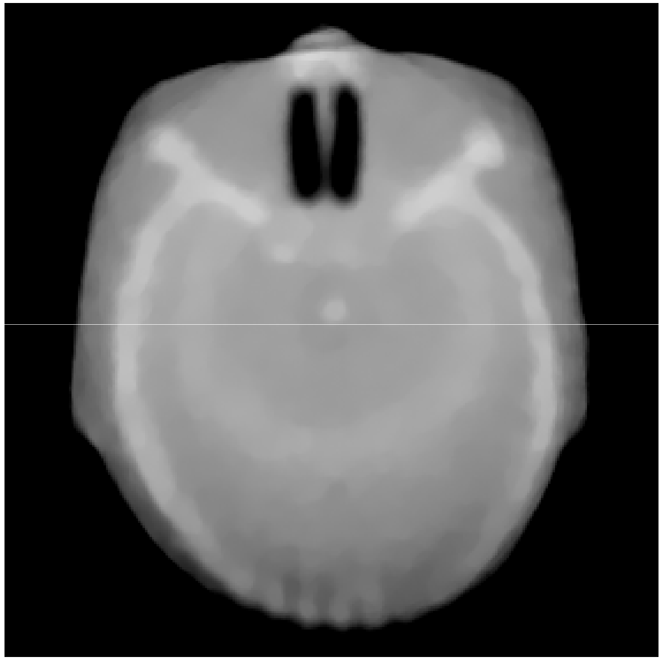

- Reconstruction based on $3.8x10^7$ proton histories
- Scan time: ~5 hours
- 200 MeV beam energy
- 90 projections (4 degree steps)
- 23 x 23 x 9 cm^3 reconstruction volume
- 384 x 384 pixels, 36 slices
  → $5.3x10^6$ voxels
- 0.6 x 0.6 mm pixel size
- 2.5 mm slice width

Image quality should be improved with a larger proton history data set.

Proton Radiography

- Proton radiographs (pRGs) showing $WEPL_{st}$ of a realistic hand phantom were obtained with 100 MeV protons
- pRGs give a more faithful representation of relative bone and soft tissue electron densities compared to x-ray RGs
- pCT RGs have also proven useful in detecting flaws in current detector designs and data processing

pCT – A low-dose image modality?

- Dose per proton & image slice (180 x 180 x 1 mm^3) of unit density: 0.67 x 0.5 nGy (<ΔE> = 100 MeV) from electronic interactions + 0.33 x 1 nGy (<ΔE> = 200 MeV) from inelastic nuclear interactions = 0.67 nGy per proton history
- Dimension of single slice head object vector: 180^2 = 3.6 x 10^4 assuming 1 x 1 x 1 mm^3 voxels
- Number of protons per slice ~ number of unknowns x10-100 ~ 3.6 x 10^5 – 3.6 x 10^6
- Average dose for a given slice: ~0.04-0.45 mGy (RBE = 1)
- Comparable to 0.07 mSv from single chest x-ray
- Even if the detection efficiency of protons is not perfect, the dose advantage of pCT compared to x-ray CT is potentially very large

0.03 mGy

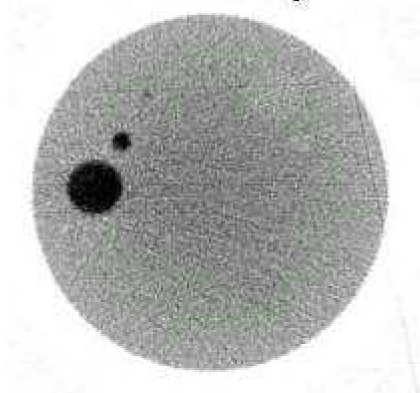

0.3 mGy

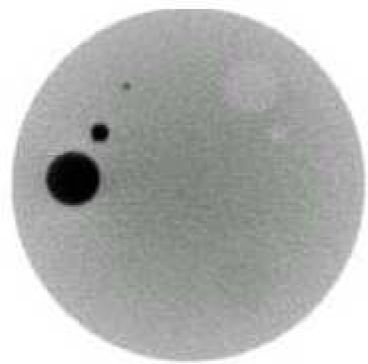

R. Schulte, Med Phys. 2005

Future Applications of pCT & pRG

- Immediate: better treatment planning in the presence of x-ray CT artifacts, e.g., from embolization glue in AVMs
- Near-term: treatment planning when very high degree of range accuracy is desired, e.g. IMpRS (intensity modulated proton radiosurgy)
- Long-term: In-room pre-treatment range verification, adapted plan of the day, low dose IGpRT
- Far future: Implementation of pretreatment pCT and intra-treatment pRG in a future multi-ion beam facility

Where to next?

- Phase II
  - Clinical scanners (9 cm x 36 cm => 9 cm x 54 cm?)
  - Faster DAQ; acquisition in less than 3 min
  - Faster Reconstruction: less than 5 min
  - Full evaluation (image quality, dose, radiobiology etc.)
- Phase II
  - Engeering of clinical hardware & control software
  - Involvement of industry
- Phase IV
  - Clinical protocol
  - Pilot testing on small number of patients
  - FDA approval

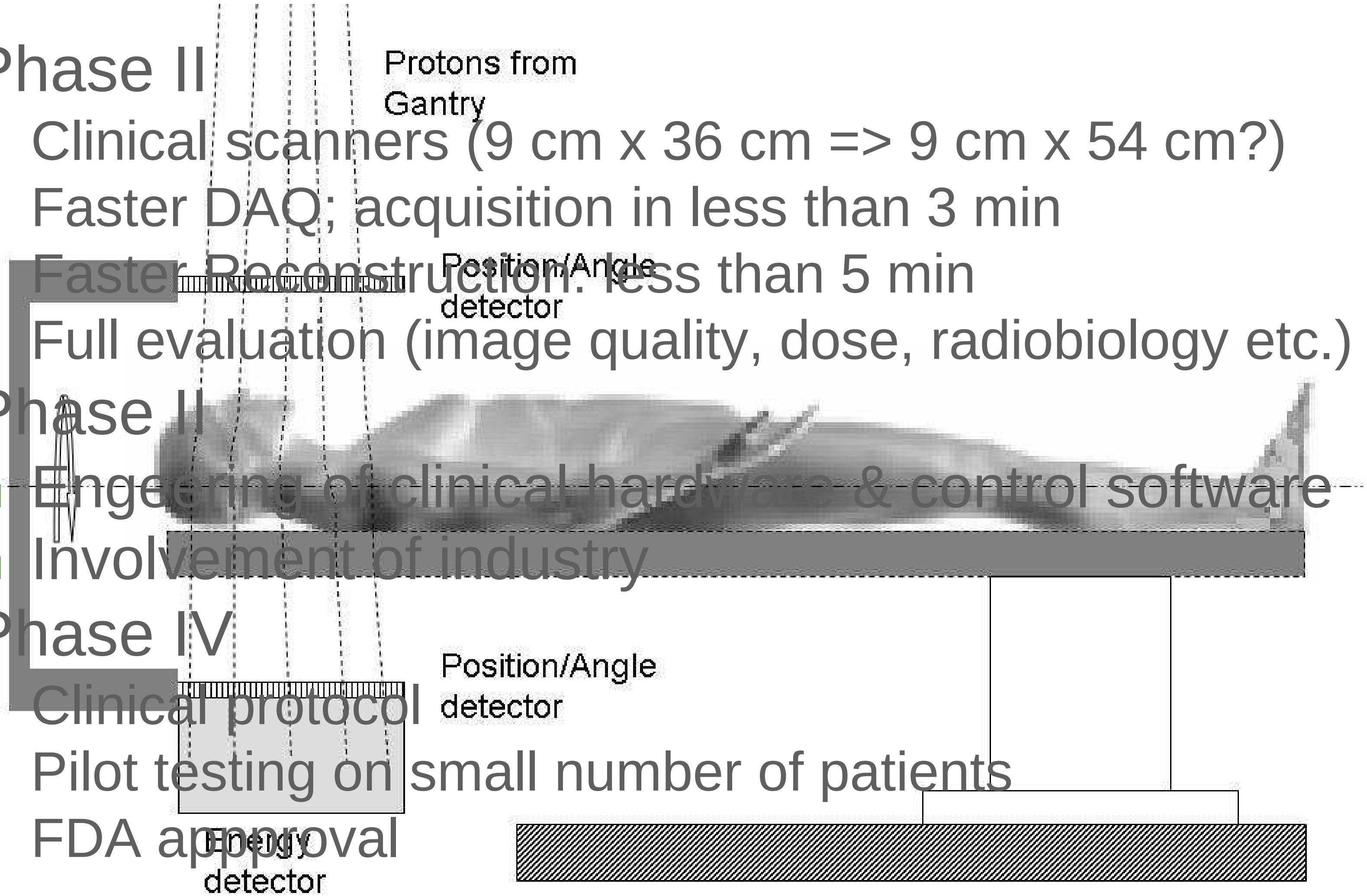

Conclusions

- pCT and pRG are evolving technologies that are driven by solving a fundamental challenge in charged particle therapy (accurate range prediction & verification)
- Fastest progress is made by continued exchange of ideas and experience between medicine, high energy & nuclear physics, applied mathematics, computer science and engineering within a framework of multi-institutional & international collaboration ("extended laboratory" concept)
- Wide-spread use can be expected within the next 10 years as proton/ion therapy expands its role in RT

Acknowledgments & Disclaimer

- pCT research is funded by a 4-year grant from the **National Institute of Biomedical Imaging** and Bioengineering (NIBIB) and the **National Science Foundatio**n (NSF), award Number R01EB013118. The content of this presentation is solely the responsibility of the authors and does not necessarily represent the official views of NIBIB, NIH and NSF. Work in pCT reconstruction has been supported by the **U.S.-Israel Binational Science Foundation** (BSF)
- The Phase 1 detectors were built at UCSC and Northern Illinois University (NIU) with support from the U.S. **Department of Defense** Prostate Cancer Research Program, award No. W81XWH-12-1-0122and the **Department of Radiation Medicine** at LLUMC (**Dr. James M. Slater**)

pCTlers

Vladimir Bashkirov
Ford Hurley
Andrew Wroe
Baron Black
Bob Jones
Hartmut Sadrozinski
Robert Johnson
Andriy Zatserklyaniy
Joel DeWitt
Forest Martinez-McKinney
Sergei Kashiguine
Edwin Spencer
Andrew Plumb
Cole Holcomb
David Steinberg
Vanessa Feng
Scott Macafee
Jessica Missaghian
Tia Plautz
Keith Schubert
Micah Witt
Blake Schultze
Reinhard Schulte
Scott McAllister
John Tafas
Yair Censor
Ran Davidi
Anatoly Rozenfeld
Peter Lazarakis
Valentina Giacometti
Carol Grande
Gerald Barnett

Gerald Blazey
George Coutrakon
Bela Erdelyi
Alexandre Dychkant
Eric Johnson
Sergey Uzunyan
Vishnu Zutshi
Karonis Nicholas
Kirk Duffin
Caesar Ordonez
John Winans
Andrew Gearhart
Mahmoud Yaqoub
Rick Salcido
Viktoriya Zvoda
Tony Zhang
Eric Olson
Michael Papka
Tom Uram
Peter Wilson
Greg Sellberg
John Rauch
John Krider
Paul Rubinov
Tom Fitzpatrick
Herman Cease
Michael Roman
Michael Utes
Anindya Sen
Gabor Herman
Scott Penfold

Márgio C. Loss Klock
Tianfang Li
Jerome Z. Liang
Ivan Evseev
Hugo Schelin
Olga Yevseyeva
Sergei Paschuk
Edney Milhoretto
Valeriy Denyak
David C. Williams
Todd Satogata
Steven Peggs
Klaus Mueller
Jason Heimann
Leah R. Johnson
Brian Keeney
David C. Williams,
Lan Zhang
Zheng Li
Craig Woody

Thank you!

LLU Radiation Research Laboratories at night (left wing & basement)